

Infrared QCD resummations at hadron colliders

A thesis submitted to the University of Manchester for the degree of
Doctor of Philosophy in the Faculty of Engineering and Physical Sciences

2011

Rosa María Durán Delgado

Particle Physics Group

School of Physics and Astronomy

Contents

1	Introduction	6
1.1	The Standard Model	7
1.2	QCD in a nutshell	8
1.3	The QCD Lagrangian	9
1.4	Hadronic cross-sections and factorization	12
1.5	Our research	14
2	Novel a_T variable for the study of Z boson production	16
2.1	Z -boson production at hadron colliders	16
2.2	Non-perturbative or “intrinsic” k_T	17
2.3	The novel a_T observable	19
2.4	Definition of a_T and soft limit kinematics	22
2.5	Born cross-section	25
2.6	Leading Order distribution	29
2.6.1	LO matrix elements	30
2.6.2	Integration over three-body phase-space	32
2.6.3	Logarithmic singularities in the a_T distribution	37
2.7	Resummation of large logarithms in a_T	42
2.7.1	The resummed exponent	46

2.8	Comparison to fixed-order results	52
2.9	Discussion and conclusions	56
3	Gaps between jets at the LHC	60
3.1	Cross-section for dijet production	64
3.2	Colour-basis independent notation	66
3.2.1	Soft gluon emission	67
3.2.2	Mapping onto a particular colour basis	70
3.3	The gap fraction	71
3.4	The resummed calculation	73
3.4.1	Non-global contribution	75
3.5	Matching	78
3.5.1	Energy-momentum conservation	82
3.6	Matched results and comparison to data	85
3.7	Discussion and conclusions	89

Word count: 85690

Abstract

Infrared QCD resummations at hadron colliders

A thesis submitted to the University of Manchester
for the degree of Doctor of Philosophy
in the Faculty of Engineering and Physical Sciences
by Rosa María Durán Delgado.

In this thesis we study two different processes at hadron colliders: Z-boson production and dijet production with a jet veto. Our calculations focus on the resummation of logarithmically enhanced contributions coming from soft and/or collinear gluon emission.

For Z-boson production, we calculate the cross-section distribution in a_T , a novel variable proposed by Vesterinen and Wyatt as a more accurate probe of the Z at low transverse momentum p_T . The observable a_T is defined as the component of p_T perpendicular to an experimentally convenient axis: the axis with respect to which the two final-state leptons (from a Z leptonic decay) have equal transverse momenta. Our study involves the resummation of large logarithms in a_T/p_T up to next-to-leading accuracy. We then compare the resulting distributions in a_T to the well-known p_T distribution, identifying important physical differences between the two cases. We also test our resummed result at the two-loop level by comparing its expansion with a fixed-order calculation and find agreement with our expectations.

Besides, we study dijet production with a veto in the inter-jet rapidity region in proton-proton collisions. We resum the leading logarithms in the ratio of the transverse momentum of the leading jets and the veto scale and we match this result to leading-order QCD matrix elements, taking into account energy-momentum conservation effects. We compare our theoretical predictions to experimental data measured by the ATLAS collaboration and find good agreement, although our results are affected by large theoretical uncertainties.

Declaration

No portion of the work referred to in this thesis has been submitted in support of an application for another degree or qualification of this or any other university or other institute of learning.

Copyright statement

i. The author of this thesis (including any appendices and/or schedules to this thesis) owns certain copyright or related rights in it (the Copyright) and she has given The University of Manchester certain rights to use such Copyright, including for administrative purposes.

ii. Copies of this thesis, either in full or in extracts and whether in hard or electronic copy, may be made only in accordance with the Copyright, Designs and Patents Act 1988 (as amended) and regulations issued under it or, where appropriate, in accordance with licensing agreements which the University has from time to time. This page must form part of any such copies made.

iii. The ownership of certain Copyright, patents, designs, trade marks and other intellectual property (the Intellectual Property) and any reproductions of copyright works in the thesis, for example graphs and tables (Reproductions), which may be described in this thesis, may not be owned by the author and may be owned by third parties. Such Intellectual Property and Reproductions cannot and must not be made available for use without the prior written permission of the owner(s) of the relevant Intellectual Property and/or Reproductions.

iv. Further information on the conditions under which disclosure, publication and commercialisation of this thesis, the Copyright and any Intellectual Property and/or Reproductions described in it may take place is available in the University IP Policy, in any relevant Thesis restriction declarations deposited in the University Library, The University Library's regulations and in The University's policy on presentation of Theses.

Acknowledgments

First, I want to thank my supervisor Jeff Forshaw for his guidance, physics insights and great support during my studies in Manchester. In these respects, I also want to thank the rest of members of the Manchester HEP group for the many interesting discussions we have as a joined theoretical and experimental team. In particular, many thanks to Mrinal Dasgupta, Simone Marzani, Mike Seymour and Fred Loebinger. I appreciate as well the financial support provided by the group.

Other physicists, not based in Manchester, have also helped me a great deal in the understanding of QCD and the use of some computational tools for the analysis of its phenomenology. Thanks to Andrea Banfi, in particular. Thanks to the group of Theoretical High Energy Physics at Lund University for giving me the motivation to continue doing research in the thrilling field of theoretical Particle Physics.

Special thanks to Hector Silva and my family. Also to my friends (Silvia Piña, Gabriel Pareyon, Jose Corrales, Paco Ríos, Jose Grima, Ana Marr, Marta Tavera, Tim Coughlin, Ira Nasteva...) that have broadened my views and helped me countless times in these last few years. Gracias.

Chapter 1

Introduction

The largest particle accelerators currently operative in the world are the *Large Hadron Collider* (LHC) at CERN, in Geneva, and the *Tevatron* at Fermilab, near Chicago. Both of them are hadron colliders. The experimental data taken from them will give us insight into the building blocks of reality as we perceive it. It will provide information about the constituents of hadrons¹, and the electromagnetic, weak and strong interactions. In principle, one could derive analytical descriptions of the physics phenomena observed at these high-energy scales. However, this can only happen if we understand the ways in which the constituents of hadrons mesh with each other. Thus, significant effort is currently devoted to improving the theory of Quantum Chromo-Dynamics (QCD), the fundamental theory of the strong force between point-like *quarks*, constituents of hadrons; and massless *gluons*, mediators of the force.

¹Hadrons are protons and neutrons (components of atomic nuclei), and other particles that can undergo strong interactions.

1.1 The Standard Model

The theory of QCD is included in the so-called Standard Model of Particle Physics, which also describes electro-weak phenomena. The Standard Model is a dynamical theory of relativistic and quantized fields, associated to a few particles, which are assumed to be elementary; its Lagrangian manifests local invariance under certain gauge transformations (see for example ref. [1] for a detailed description of the theory).

Let me briefly explain the ideas that lead to the construction of the Standard Model. In the realms of Particle Physics we cannot neglect the effects that occur at short distances and at high speeds. These counter-intuitive effects are described by Quantum Mechanics and Special Relativity, so both theories are taken into account in the Standard Model of Particle Physics. Besides, physics phenomena always seem to manifest symmetries: some quantity remains unchanged in any physical process. Symmetries thus constitute the core around which the Standard Model is built.

The Lagrangian of the Standard Model arises almost naturally by following these ideas. The resulting expression is rather condensed and elegant from a mathematical point of view, while at the same time it has proven to be very successful at describing many observables at particle colliders. Perhaps even more interesting is the fact that the theory includes, in its simple Lagrangian, physics from nuclear and atomic scales, as well as the classic Maxwell equations of electromagnetism, patent in our day-to-day experience.

Let us now introduce some key ideas of QCD, before describing our calculations.

1.2 QCD in a nutshell

In summary, QCD is a $SU(3)$ non-Abelian gauge theory that has shown good agreement with a large body of data taken mainly from particle colliders (see [2] and references therein).

According to this theory, each quark (quarks are the constituents of hadrons) takes one out of three possible charges, illustratively named *colours*, and always manifests in nature combined with other quarks into colour-singlet states. This is an important element of the theory, it is the property known as *colour confinement*.

QCD also embodies the idea that quarks behave as free particles in processes involving short distance/time scales, associated with large momentum transfers. Phenomena can be appropriately described in these realms through perturbative techniques, like those used in the calculation of electromagnetic observables from the simpler gauge-field theory of Quantum Electrodynamics. This second property is known as *asymptotic freedom*.

The quantum field theory of QCD is capable of explaining this rather strange behaviour of the strong interaction. The properties of asymptotic freedom and quark confinement can be inferred from the dynamic content of the theory, i.e. from its Lagrangian, which will be reviewed in next section.

Let us now see how QCD describes the dependence of the strong coupling on the energy of a scattering event. The quantum-field theory of QCD needs to be renormalized if one wants to get rid of unphysical ultraviolet divergences. In this renormalization procedure we need to introduce an arbitrary mass scale, known as a *renormalization* scale. Since physical observables (calculated in a perturbation series of the coupling $\alpha_s = g^2/4\pi$) cannot depend on this scale, the renormalized *running* coupling must include some dependence on the cut-off scale (see the details

in Ref. [2]).

The dependence of the strong coupling $\alpha_s = g^2/4\pi$ on the renormalization scale Q^2 is given by

$$\frac{d\alpha_s}{d\ln Q^2} = \beta(\alpha_s(Q^2)) = -\alpha_s(Q^2) [\beta_0\alpha_s(Q^2) + \beta_1\alpha_s^2(Q^2) + \dots] \quad (1.1)$$

where the beta function coefficients are defined as [2]

$$\beta_0 = \frac{11C_A - 2n_f}{12\pi}, \quad \beta_1 = \frac{17C_A^2 - 5C_An_f - 3C_Fn_f}{24\pi^2}, \quad (1.2)$$

n_f being the number of active quark flavours, $C_F = 4/3$ the colour factor associated with gluon emission from a quark and $C_A = 3$ the colour factor associated with gluon emission from a gluon.

The two-loop coupling equation (used throughout this thesis), running from energy scale M^2 to Q^2 , is given by

$$\alpha_s(Q^2) = \frac{\alpha_s(M^2)}{1 - \rho} \left[1 - \alpha_s(M^2) \frac{\beta_1 \ln(1 - \rho)}{\beta_0} \frac{1}{1 - \rho} \right], \quad \rho = \alpha_s(M^2) \beta_0 \ln \frac{M^2}{Q^2}. \quad (1.3)$$

We see that the coupling increases at decreasing scales and gets weaker as the momentum increases. The rate of decrease of α_s is slow though (falling as $\ln^{-1} Q^2$) and one often needs to include corrections to leading order perturbative results. Moreover, as the coupling becomes large at small scales, perturbation theory is no longer valid and one needs non-perturbative input, for example the so-called parton-distribution functions, as we will see in section 1.4.

1.3 The QCD Lagrangian

The perturbative QCD Lagrangian density is given by

$$\mathcal{L}_{QCD} = \sum_{flavours} \bar{q}(x)(i\gamma^\mu D_\mu - m)q(x) - \frac{1}{2}\text{Tr}[F_{\mu\nu}(x)F^{\mu\nu}(x)] + \mathcal{L}_{GF} + \mathcal{L}_{ghost}. \quad (1.4)$$

Hereafter we will neglect the contributions of the gauge fixing \mathcal{L}_{GF} and ghosts \mathcal{L}_{ghost} terms; they are introduced to properly quantize the theory, but the details are beyond the scope of this thesis.

The first term (a sum over quark flavours) gives rise to the usual Dirac equation for the quarks. We represent each quark by $q(x)$, an N -tuple of relativistic fermion fields, where N is the number of colours $N \equiv N_c = 3$. The components of the N -tuple represent different states of the quark, all of them having the same mass m , but different colours.

The dynamics of the spin-1 gluon fields is given by the second term

$$-\frac{1}{2}\text{Tr}[F_{\mu\nu}(x)F^{\mu\nu}(x)]. \quad (1.5)$$

Like in the electromagnetic theory, we define the field strength tensor F in terms of the gauge field, as

$$F_{\lambda\rho}(x) = D_\lambda G_\rho(x) - D_\rho G_\lambda(x). \quad (1.6)$$

In QCD the gauge field is the colour-octet field of the gluon $G_\mu(x) = G_\mu^a(x)t_a$. It contains the gluon four-potentials, $G_\lambda^a(x)$, $a = 1, \dots, 8$. t_a represents the colour charge. The properties of the colour matrices $t_a \equiv \lambda_a/2$ are important in what follows, so we summarize them:

$$[\lambda_a/2, \lambda_b/2] = if_{abc}\lambda_c/2, \quad (1.7)$$

f_{abc} are totally antisymmetric in a, b, c , and are called the structure constants. Equation (1.7) defines the Lie algebra of the group. The normalization is usually chosen so that $\text{Tr}(\lambda_a\lambda_b) = 2\delta_{ab}$. Then the colour matrices satisfy the following relations:

$$\sum_a t_a^{ij} t_a^{jk} = C_F \delta_{ik}, \quad C_F = \frac{N^2 - 1}{2N} = \frac{4}{3}, \quad (1.8)$$

$$\sum_{a,b} f_{abc} f_{abd} = C_A \delta_{cd}, \quad C_A = N = 3. \quad (1.9)$$

Equation (1.4) is obtained from the requirement of gauge invariance of the theory. The Lagrangian needs to be invariant under the following transformations of the quark and gauge fields respectively:

$$q(x) \rightarrow U(x)q(x) \quad (1.10)$$

$$F_{\mu\nu} \rightarrow UF_{\mu\nu}U^\dagger, \quad (1.11)$$

with

$$U(x) = e^{i\omega_a(x)t_a}. \quad (1.12)$$

$U(x)$ is a $N \times N$ matrix, hermitian and traceless, which must include the identity matrix; in other words, $U(x) \in SU(3)$. Thus, the invariant transformation of the fermion field is just a $SU(N_c)$ rotation through ω , the colour matrices t_a being the $N_c^2 - 1$ generators of the rotation.

Note that the requirement of gauge invariance of the Lagrangian implies that the operator D_μ cannot simply be the usual covariant derivative ∂_μ . D_μ is instead given by

$$D_\mu = \mathbf{1} \partial_\mu + i g_s G_\mu(x), \quad (1.13)$$

where g_s is the dimensionless strong coupling constant. This is the minimal substitution of the derivative operator that guarantees gauge invariance. Inserting D_μ in Eq. (1.6) and then into the Lagrangian, we find explicitly the terms that describe the triplet and quartic gluon self-interactions. These ‘non-Abelian’ terms are ultimately responsible for the property of asymptotic freedom.

Likewise, the term $-g_s \bar{q} \gamma^\mu G_\mu^a t_a q$ is implicit in the Lagrangian with the definition of D_μ in expression (1.13). This term describes the ‘minimal interaction’

between gluons and quarks. The interaction between one gluon and two quarks is thus explained in the theory as a mere consequence of gauge invariance.

1.4 Hadronic cross-sections and factorization

The formula that we will use to calculate hadronic cross-sections is the following:

$$d\sigma_{h_1 h_2 \rightarrow X} = \sum_{i,j} \int_0^1 \int_0^1 f_i(x_1, \mu^2) f_j(x_2, \mu^2) d\hat{\sigma}_{ij \rightarrow X}(Q^2/\mu^2) dx_1 dx_2 . \quad (1.14)$$

We consider the hard scattering as if it was simply initiated by any two partons (quarks or gluons) of type i, j . The *parton distribution functions* (pdfs) $f_i(x, \mu^2)$ are the number densities of partons of type i carrying a fraction x of the longitudinal momentum of the incoming hadrons, when resolved at a *factorization* scale μ , and $d\hat{\sigma}_{ij \rightarrow X}$ are the partonic contributions to the cross-section. The pdfs include in their definition the emission of quarks and gluons from the original partons when they are emitted with some transverse momentum below the factorization scale; this is known as initial-state collinear radiation. The factorization scale is an arbitrary parameter that we set to separate long- and short-distance components of the cross section; practically speaking it should be chosen of the order of the hard scale that characterizes the process. The pdfs are universal (independent of the type of scattering but dependent on the type of incoming particle) and they have values taken from experiment. Their evolution in terms of the scale μ^2 can be calculated perturbatively through the DGLAP equations [3–6].

If the cross-section is defined in terms of final-state hadrons then one also needs to convolute the partonic cross-sections with fragmentation functions, to include the effects of hadronization. We will not be considering such observables in this thesis.

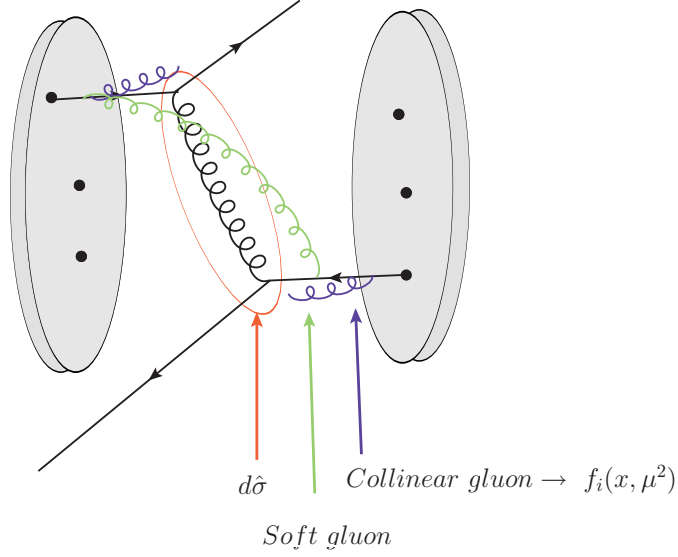


Figure 1.1: Typical QCD event with a hard partonic interaction marked in red, initial-state gluon collinear emission in blue and soft gluon virtual radiation illustrated in green.

Hence we see explicitly a factorization of long and short distance physics in Eq.(1.14). The factorization theorem expresses the idea that the soft colour field generated by the incoming hadrons does not affect the probability for the hard collision. However, at each order in the perturbative series of our QCD calculations large logarithmic terms arise from gluons whose momentum components are all small compared with the scale of the scattering [8]. These *soft gluons* cannot generally be factorized into the pdfs; instead they are calculated as corrections to the primary hard scattering and they are included in $d\hat{\sigma}$. In our body of work we will study the impact of soft gluon emission on the cross-sections of two different hadronic-scattering scenarios, Z-boson production and gaps between jets.

1.5 Our research

In this thesis we focus on two particular scenarios that can give us insight in the understanding of the infrared sector of QCD: Z-boson production, via the channel $hh \rightarrow Z \rightarrow ll$, and dijet events with a jet veto within the rapidity interval between the two jets.

In the former type of event, the kinematics of the produced Z boson can be precisely determined from its particular clean decay to a pair of charged leptons. In the spectrum of its transverse momentum p_T , specifically at low values, we find contributions coming from non-perturbative QCD radiation. These non-perturbative effects are universal and therefore expected to be present also in events involving new physics, such as the production of SUSY particles or the Higgs boson. However, this region of the p_T distribution is highly sensitive to experimental systematics, and the data available are not yet precise enough to accurately constrain the modeling of the non-perturbative effects. In this context, we provide the first theoretical study of a novel variable a_T , proposed in Ref. [9] as a more accurate probe of the region of low transverse momentum p_T . Our calculation of the a_T distribution for Z-boson production at hadron colliders (which involves resummation of large logarithms in a_T) will be presented in Chapter 2.

The second process that we study can also give us much information on the role of soft gluons in QCD: it is dijet production in proton-proton collisions with a veto on the emission of a third jet in the rapidity region in between the two leading ones. In Chapter 3, we explain our calculation for its cross-section. In short, we make a soft-gluon resummation of the most important logarithms in the ratio of the transverse momentum of the leading jets and the veto scale. We include leading logarithms and a (partial) tower of non-global logarithms coming from the

emission of one gluon outside the gap. Then we match this result to leading-order QCD matrix elements. We find that, in order to obtain sensible results, we have to modify the resummation and take into account energy-momentum conservation effects. We compare our theoretical predictions for the gap fraction to experimental data measured by the ATLAS collaboration and find good agreement, although our results are affected by large theoretical uncertainties. We then discuss differences and similarities of our calculation to other theoretical approaches.

Chapter 2

Novel a_T variable for the study of Z boson production

2.1 Z -boson production at hadron colliders

The production of W and Z bosons at hadron colliders via the Drell-Yan process [2] has formed a very significant part of particle phenomenology almost since their discovery [10–12]. In the era of the LHC these studies continue to occupy an important role for a variety of reasons. For instance, an accurate understanding of the production rates and p_T distributions of the W and Z can be used for diverse purposes which range from more prosaic applications such as luminosity monitoring at the LHC to measurement of the W mass and perhaps most interestingly for discovery of new physics, which may manifest itself via the decay of new gauge bosons to lepton pairs.

In particular, the p_T spectrum of the Z/γ^* bosons (denoted simply as “ Z bosons” throughout this thesis) has received considerable theoretical and experimental attention in the past, but there remain aspects where it is desirable to have

an improved understanding of certain physical issues. One such important issue is the role of the non-perturbative or “intrinsic” k_T component (explained in the following section) which may have a sizable effect on the p_T spectrum at low p_T (see e.g Refs. [13–15]).

For the precise determination of p_T spectra at the LHC, it is important to have as thorough a probe of the low p_T region of Z -boson production as it is possible. Investigations carried out using the conventional p_T spectrum mainly suffer from large uncertainties arising from experimental systematics, dominated by resolution unfolding and the dependence on p_T of event selection efficiencies, as represented in Fig. 2.1 and discussed in detail in Ref. [9].

2.2 Non-perturbative or “intrinsic” k_T

The incoming quarks/anti-quarks which partake in any event at the Tevatron or LHC hadron colliders are part of extended objects (protons or anti-protons) and have interactions with other constituents thereby generating a small transverse momentum k_T . This transverse momentum can be viewed as the Fermi motion of partons inside the proton and a priori one might expect it to be of order of the QCD scale Λ_{QCD} .

Since the intrinsic k_T has a non-perturbative origin it cannot be computed within conventional methods of perturbative QCD. One can however model the intrinsic k_T as an essentially Gaussian smearing of the perturbatively calculated p_T spectra and hope to constrain the parameters of the Gaussian by fitting the theoretical prediction to experimental data. An example of this procedure is provided by the work of Brock, Landry, Nadolsky and Yuan (BLNY). Their proposed non-perturbative Gaussian form factor in conjunction with perturbative calcula-

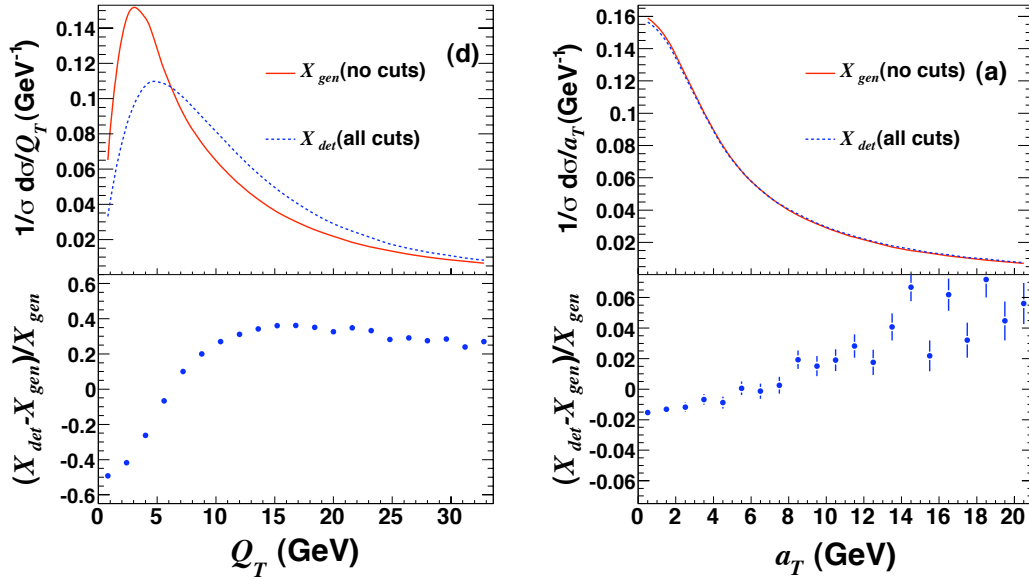


Figure 2.1: Monte Carlo simulations of the generator and detector level distributions at the Run II D \emptyset detector for (left) the Z boson transverse momentum p_T and (right) the novel variable a_T described in next section. The detector level distributions are for Gaussian smearing in $1/Q_T \equiv 1/p_T$ of width 0.003 GeV^{-1} (which simulates the imperfect lepton p_T resolution of the detector), and all selection cuts are applied. The generator level distributions do not include selection cuts. The lower halves of each plot show the fractional differences. *Figures from Ref. [9].*

tions was able to describe both Tevatron Run-1 Z data as well as Drell-Yan data corresponding to lower scattering energies [15]. Alternatively to this procedure, one may also use a Monte Carlo event generator such as HERWIG++ [16] to investigate this issue. As discussed in Ref. [17] these studies yield k_T values somewhat larger than expected and also reveal a dependence of this quantity on the collider energy, which features are desirable to understand better.

Additionally, as pointed out by Berge et al. [18], studies from semi-inclusive DIS events at the HERA- ep collider suggest a *small- x broadening* of their form factor, for small Bjorken- x values ($x < 10^{-3}$).¹ Extrapolating the effect to the LHC where such small- x values become relevant, one may expect to see significantly broader Higgs and vector boson p_T spectra than one would in the absence of small- x effects [18]. Berge et al. suggested that Tevatron studies with samples of vector-boson with high rapidities would help to provide further information on the role, if any, of the small- x broadening on non-perturbative parameters. The DØ Run II data on p_T [20] was not particularly sensitive to such broadening at low p_T (see Fig. 2.2) and more precision is required to reach any conclusion.

2.3 The novel a_T observable

We have seen that the low values of p_T of Z bosons produced at hadron colliders form a distribution particularly interesting for the understanding of non-perturbative effects. However, the measured p_T is highly sensitive to experimental systematics, in particular to the transverse-momentum resolution of the leptons

¹This x dependence may be merely an effective parametrisation of missing *perturbative* BFKL effects. Another observable was suggested in Ref. [19] to investigate this x dependence: the p_T -component in one hemisphere in the DIS Breit frame.

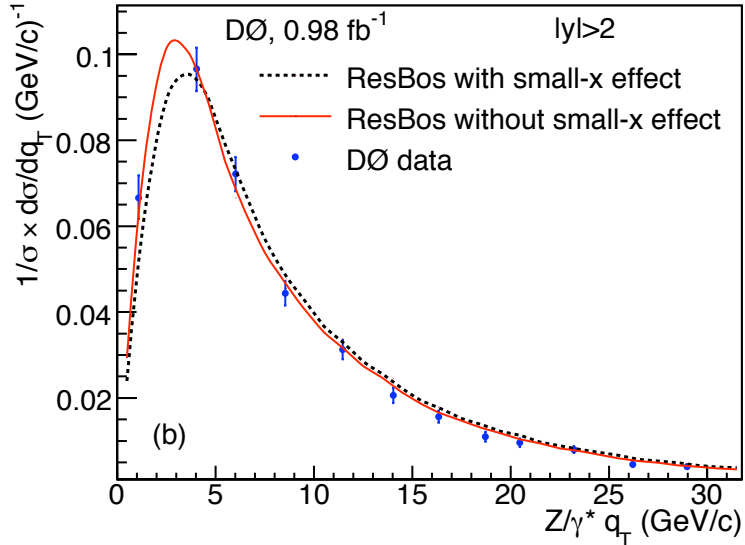


Figure 2.2: Normalized Z boson transverse momentum distributions. The points are the D0 Run II data, the solid curve is the ResBos prediction and the dashed line is the prediction from the form factor modified after studies of small- x DIS data. ResBos [21] is an event generator which incorporates a resummation at all perturbative orders for low p_T , including the BLNY non-perturbative form factor, and then matches it to a fixed order NLO perturbative calculation for high p_T . *Figure published in Ref. [20].*

produced by the Z boson and also to the overall event selection efficiency.

An alternative observable to study the low Z p_T region should ideally be less sensitive to experimental systematic errors, whilst still sensitive to the Z boson p_T . Keeping in mind that collider detectors generally have far better angular resolution than calorimeter transverse momentum track resolution, an observable satisfying both of these requirements was proposed in Ref. [9]. This variable, a_T , is defined as the transverse component with respect to the lepton thrust axis. From Fig. 2.1 (published in Ref. [9]) it is clear that a_T is experimentally better determined at low values than the standard p_T variable and hence it would make a more accurate

probe for our understanding of non-perturbative effects.

Before one can access information on non-perturbative effects, however, it is of vital importance to have a sound perturbative estimate of the observable at hand. In the low p_T region we need to deal with the emission of soft and/or collinear gluons which is logarithmically enhanced. The resummation of large logarithms of the form $1/p_T [\alpha_s^n \ln^m(M^2/p_T^2)]$, where M is the lepton-pair invariant mass and $m \leq 2n - 1$, has been a subject of interest over decades [21–26] and has now been carried out to next-to-next-to leading logarithmic (NNLL) accuracy [27]. After matching such resummations with fixed-order estimates to NLO accuracy one has a state-of-the-art theoretical prediction for the perturbative region.

Following these lines, we have performed a theoretical study of a_T (published in [28]), which we present as follows: we begin by discussing the definition of a_T and its dependence on multiple soft gluon emission which is important at low a_T , where one encounters large logarithms. In the following section we sketch a leading-order calculation for the a_T distribution, which helps to illustrate some features such as the precise origin of logarithmically enhanced terms. In the subsequent section we carry out a resummation of the logarithms of a_T to NLL accuracy pointing out the relation to a recent study on azimuthal jet decorrelations [30]. Next we identify a relationship between the a_T and p_T distributions at fixed order and check this relationship with the help of a numerical fixed-order calculation using the program MCFM [31], which is a non-trivial test of our resummation. We conclude by pointing out the possibilities for further work which involve an extension of our resummation to NNLL accuracy as well as matching to the MCFM results and phenomenological investigation once final experimental data become available.

2.4 Definition of a_T and soft limit kinematics

We are concerned in this chapter with large logarithms in the perturbative description of the a_T variable and their resummation. Since these logarithms have their origin in multiple soft and/or collinear emissions from the incoming hard partons we need to derive the dependence of a_T on such emissions. In this section therefore we define a_T and obtain its dependence on the small transverse momenta k_t of emissions.

We are considering the production of Z bosons via the Drell-Yan (and QCD Compton) mechanisms which subsequently decay to a lepton pair. The a_T is the component of the lepton pair (or equivalently Z boson) p_T transverse to a suitably defined axis, sketched in Fig.2.3. The precise definition of the lepton thrust axis

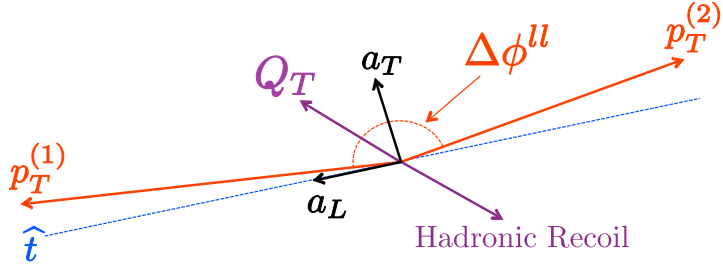


Figure 2.3: Schematic representation in the transverse plane, of the novel a_T observable, where Q_T in the figure represents the standard transverse momentum p_T of a Z boson decaying leptonically. *Figure from Ref. [9].*

as employed in Ref. [9] is provided below:

$$\hat{n} = \frac{\vec{p}_{t1} - \vec{p}_{t2}}{|\vec{p}_{t1} - \vec{p}_{t2}|}, \quad (2.1)$$

where \vec{p}_{t1} and \vec{p}_{t2} are the transverse momenta of the two leptons and thus \hat{n} is a unit vector in the plane transverse to the beam direction. It is straightforward

to verify that this is the axis with respect to which the two leptons have equal transverse momenta.

We now consider multiple emissions from the incoming partons which (neglecting the intrinsic k_T) are back-to-back along the beam direction. From conservation of transverse momentum we have $\vec{p}_{t1} + \vec{p}_{t2} = -\sum_i \vec{k}_{ti}$ which means that the lepton pair or Z boson p_T is just minus the vector sum of emitted gluon transverse momenta \vec{k}_{ti} , where we refer to the momentum transverse to the beam axis. To obtain the dependence of a_T on the k_{ti} we wish to find the component of this sum normal to the axis defined in eq. (2.1). The axis is given by (writing \vec{p}_{t2} in terms of \vec{p}_{t1} and \vec{k}_{ti})

$$\hat{n} = \frac{2\vec{p}_{t1} + \sum_i \vec{k}_{ti}}{|2\vec{p}_{t1} + \sum_i \vec{k}_{ti}|} \approx \frac{\vec{p}_{t1}}{|\vec{p}_{t1}|}, \quad (2.2)$$

where to obtain the last equation we have neglected the dependence of the axis on emissions k_{ti} . The reason for doing so is that we are projecting the vector sum of the k_{ti} along and normal to the axis and any term $\mathcal{O}(k_{ti})$ in the definition of the axis impacts the projected quantity only at the level of terms bilinear or quadratic in the small k_{ti} . Such terms can be ignored compared to the leading linear terms $\sim k_{ti}$ that we shall retain and thus to our accuracy the axis is along the lepton direction.²

We can parametrise the lepton and gluon momenta in the plane transverse to the beam as below:

$$\begin{aligned} \vec{p}_{t1} &= p_t (1, 0) \\ \vec{k}_{ti} &= k_{ti} (\cos \phi_i, \sin \phi_i), \end{aligned} \quad (2.3)$$

²To be more precise the recoil of the axis against soft emissions, if retained, corrects our result only by terms that vanish as $a_T \rightarrow 0$. Such terms are beyond the scope of NLL resummation but will be included up to NLO due to the matching.

where ϕ_i denotes the angle made by the i^{th} emission with respect to the direction of lepton 1 in the transverse plane. It is thus clear that, expressed in these terms, the transverse component of the Z boson p_T is simply $-\sum_i k_{ti} \sin \phi_i$ ³ and one has

$$a_T = \left| \sum_i k_{ti} \sin \phi_i \right|. \quad (2.4)$$

We note immediately that the dependence on soft emissions is identical to the case of azimuthal angle $\Delta\phi$ between final state dijets near the back-to-back region $\Delta\phi \approx \pi$, for which resummation was carried out in Ref. [30]. This is not surprising since the component of the Z boson p_T , transverse to the axis defined above, is proportional in the soft limit to $\pi - \Delta\phi$, where $\Delta\phi$ is the angle between the leptons in the plane transverse to the beam. The other (longitudinal) component of Z boson p_T , a_L , is proportional to $p_{t1} - p_{t2}$ the difference in lepton squared transverse momenta.⁴ Since it is possible to measure more accurately the lepton angular separation compared to their p_t imbalance (where momentum resolution is an issue), one can obtain more accurate measurements of a_T as compared to a_L or the Z boson p_T which is given by $\sqrt{a_T^2 + a_L^2}$ [9]. The resummation that we carry out in next section will be similar in several details to those of Refs. [30, 32] but simpler since the final state hard particles are colourless leptons.

In the following sections we shall study the integrated cross-section which is directly related to the number of events below some fixed value of a_T

$$\Sigma(a_T, M^2) = \int_0^{a_T} \frac{d^2\sigma}{da'_T dM^2} da'_T, \quad (2.5)$$

³The resummation for the variable $E_T = \sum_i k_{ti}$ was performed in [29].

⁴For the case of dijet production the leptonic p_t imbalance has also been addressed via resummation in Ref. [32] which to our knowledge is the first extension of the p_T resummation formalism to observables involving final state jets.

from which the distribution in a_T can be obtained by differentiation and the dependence of Σ on M^2 will be henceforth implied. We shall first review the Born cross-section of the Drell-Yan process, which needs to be included in the total cross-section defined in eq. (2.5). We will also compute the single and double logarithmically enhanced terms in a_T and relate them to the corresponding logarithms in the standard p_T distribution at leading order in α_s . The discussion here should facilitate an understanding of the resummation we carry out in the next section and the results of subsequent sections.

2.5 Born cross-section

At Born level we have to consider the *Drell-Yan* process $p_1 + p_2 = l_1 + l_2$ where p_1, p_2 and l_1, l_2 are the four momenta of incoming partons and outgoing leptons respectively, the lepton pair being produced via Z decay. At this level the p_T of the lepton pair and hence a_T vanishes, so that the full Born result, evaluated at fixed mass M^2 , contributes to the cross-section in Eq. (2.5).

The Born cross section can be calculated from the following equation:

$$\begin{aligned} \Sigma^{(0)}(M^2) = & \int_0^1 dx_1 \int_0^1 dx_2 [f_q(x_1)f_{\bar{q}}(x_2) + q \leftrightarrow \bar{q}] \times \\ & \times \int d\Phi(l_1, l_2) \mathcal{M}_{\text{DY}}^2(l_1, l_2) \delta(M^2 - 2l_1.l_2) , \quad (2.6) \end{aligned}$$

where x_1 and x_2 are momentum fractions carried by partons p_1 and p_2 of the parent hadron momenta, $f_q(x_1)$ and $f_{\bar{q}}(x_2)$ denote parton distribution functions⁵, $d\Phi(l_1, l_2)$ is the two-body phase-space, and $\mathcal{M}_{\text{DY}}^2$ is the Born matrix element given

⁵In order to avoid excessive notation we do not explicitly indicate the sum over incoming parton flavours which should be understood.

by [33]

$$\mathcal{M}_{\text{DY}}^2(l_1, l_2) = \frac{8}{N_c} \mathcal{G}(\alpha, \theta_W, M^2, M_Z^2) [A_l A_q (t_1^2 + t_2^2) + B_l B_q (t_1^2 - t_2^2)]. \quad (2.7)$$

The electroweak coefficient constants \mathcal{G} , A_l , A_q , B_l , B_q for the case of Z boson exchange are:

$$\begin{aligned} \mathcal{G}(\alpha, \theta_W, M^2, M_Z^2) &= \frac{4\pi^2 \alpha^2}{\sin^4 \theta_W \cos^4 \theta_W} \frac{1}{(M^2 - M_Z^2)^2 + (\Gamma_Z M_Z)^2}, \\ A_f &= a_f^2 + b_f^2, \quad B_f = 2a_f b_f, \quad (f = l, q). \end{aligned} \quad (2.8)$$

All these quantities have been taken from Ref. [33], where the reader can find analogous expressions for the case in which a virtual photon is exchanged as well.

Following the conventions of Ref. [33], we also have

$$\begin{aligned} a_l &= -\frac{1}{4} + \sin^2 \theta_W, & b_l &= \frac{1}{4}, \\ a_{u,c} &= \frac{1}{4} - \frac{2}{3} \sin^2 \theta_W, & b_{u,c} &= -\frac{1}{4}, \\ a_{d,s,b} &= -\frac{1}{4} + \frac{1}{3} \sin^2 \theta_W, & b_{d,s,b} &= \frac{1}{4}. \end{aligned} \quad (2.9)$$

Henceforth we shall suppress the dependence of \mathcal{G} , which has dimension M^{-4} , on the standard electroweak parameters α, θ_W, M_Z . The factor $1/N_c$ comes from the average over initial state colours.

We have also defined the invariants⁶

$$t_1 = -2p_1 \cdot l_1 \quad t_2 = -2p_2 \cdot l_1, \quad (2.10)$$

while M^2 is the invariant mass of the lepton pair which we fix. The component $t_1^2 + t_2^2$ is the parity conserving piece also present in the case of the virtual photon

⁶The quantities t_1 and t_2 were labeled as \hat{t}_1, \hat{t}_2 while l_1 and l_2 were labeled k_1 and k_2 in Ref. [33].

process while the $t_1^2 - t_2^2$ component is related to the parity violating piece of the electroweak coupling and hence absent for the photon case.

We now look at the Lorentz-invariant phase-space which can be written as

$$\int d\Phi(l_1, l_2) = \frac{1}{2\hat{s}} \int \frac{d^3l_1}{2(2\pi)^3 l_{10}} \frac{d^3l_2}{2(2\pi)^3 l_{20}} (2\pi)^4 \delta^4(p_1 + p_2 - l_1 - l_2), \quad (2.11)$$

where \hat{s} is the partonic centre of mass energy squared $\hat{s} = s x_1 x_2$. Note that in addition to the usual two-body phase space we included a delta function corresponding to holding the invariant mass of the lepton-pair at M^2 .

We parameterise the four vectors of the incoming partons and outgoing leptons as below (in the lab frame)

$$\begin{aligned} p_1 &= \frac{\sqrt{s}}{2} x_1 (1, 0, 0, 1), \\ p_2 &= \frac{\sqrt{s}}{2} x_2 (1, 0, 0, -1), \\ l_1 &= l_T (\cosh y, 1, 0, \sinh y), \end{aligned} \quad (2.12)$$

with l_2 being fixed by the momentum conserving delta function.

In the above \sqrt{s} denotes the centre of mass energy of the incoming hadrons, while l_T and y are the transverse momentum and rapidity of the lepton with respect to the beam axis and we work in the limit of vanishing lepton and quark masses. In these terms we can express Eq. (2.11) as (after integrating over l_2 using the momentum conserving delta function)

$$\int d\Phi(l_1, l_2) = \frac{1}{2\hat{s}} \int \frac{l_T dl_T dy}{4\pi} \delta((p_1 + p_2 - l_1)^2), \quad (2.13)$$

where we have carried out an irrelevant integration over lepton azimuth. Note that the factor $\delta((p_1 + p_2 - l_1)^2)$ arises from the vanishing invariant mass of lepton l_2 .

In order to obtain the full Born result we need to fold the above phase-space with the parton distribution functions and the squared matrix element for the

Drell-Yan process to obtain

$$\begin{aligned} \Sigma^{(0)}(M^2) &= \int_0^1 dx_1 f(x_1) \int_0^1 dx_2 f(x_2) \times \\ &\quad \times \frac{1}{2\hat{s}} \int \frac{l_T dl_T dy}{4\pi} \delta(s x_1 x_2 + t_1 + t_2) \delta(M^2 - x_1 x_2 s) \mathcal{M}_{\text{DY}}^2, \end{aligned} \quad (2.14)$$

where we used $(p_1 + p_2 - l_1)^2 = s x_1 x_2 + t_1 + t_2$.

We next evaluate the squared matrix element $\mathcal{M}_{\text{DY}}^2$ in Eq. (2.7) in terms of the phase space integration variables, using:

$$t_1 = -2p_1 \cdot l_1 = -\sqrt{s} x_1 l_T e^{-y}, \quad t_2 = -\sqrt{s} x_2 l_T e^y. \quad (2.15)$$

Inserting these values of t_1 and t_2 in Eq. (2.14) we use the constraint

$$\delta(s x_1 x_2 + t_1 + t_2) = \delta(s x_1 x_2 - \sqrt{s} l_T (x_2 e^y + x_1 e^{-y})), \quad (2.16)$$

to carry out the integration over l_T which gives

$$\frac{1}{8\pi s} \int_0^1 dx_1 f(x_1) \int_0^1 dx_2 f(x_2) \delta(M^2 - x_1 x_2 s) \frac{dy}{(x_2 e^y + x_1 e^{-y})^2} \mathcal{M}_{\text{DY}}^2, \quad (2.17)$$

where in evaluating $\mathcal{M}_{\text{DY}}^2$ one needs to use $l_T = \sqrt{s} x_1 x_2 / (x_2 e^y + x_1 e^{-y})$, which yields using (2.15)

$$\begin{aligned} t_1^2 &= x_1^2 e^{-2y} \frac{M^4}{(x_2 e^y + x_1 e^{-y})^2}, \\ t_2^2 &= x_2^2 e^{2y} \frac{M^4}{(x_2 e^y + x_1 e^{-y})^2}. \end{aligned} \quad (2.18)$$

Using the above to evaluate $\mathcal{M}_{\text{DY}}^2$ in (2.7) we obtain

$$\Sigma^{(0)}(M^2) = \frac{\mathcal{G}}{N_c} \frac{M^4}{\pi s} \int_0^1 dx_1 f(x_1) \int_0^1 dx_2 f(x_2) \delta(M^2 - x_1 x_2 s) \int dy \mathcal{F}(x_1, x_2, y), \quad (2.19)$$

where we introduced

$$\mathcal{F}(x_1, x_2, y) = A_l A_q \frac{x_1^2 e^{-2y} + x_2^2 e^{2y}}{(x_2 e^y + x_1 e^{-y})^4} + B_l B_q \frac{x_1^2 e^{-2y} - x_2^2 e^{2y}}{(x_2 e^y + x_1 e^{-y})^4}. \quad (2.20)$$

Integrating the angular function \mathcal{F} over rapidity over the full rapidity range⁷ one finds as expected that the parity violating component proportional to $B_l B_q$ vanishes and the result is $A_l A_q/(3x_1 x_2)$. Thus the final result is (using $x_1 x_2 = M^2/s$)

$$\begin{aligned} \Sigma^{(0)} &\equiv \Sigma^{(0)}(M^2) = \\ &= \mathcal{G} \frac{M^2}{3\pi} \frac{A_l A_q}{N_c} \int_0^1 dx_1 \int_0^1 dx_2 [f_q(x_1) f_{\bar{q}}(x_2) + q \leftrightarrow \bar{q}] \delta(M^2 - s x_1 x_2) . \end{aligned} \quad (2.21)$$

2.6 Leading Order distribution

We now derive the QCD corrections to leading order in α_s with the aim of identifying logarithmically enhanced terms in a_T to the integrated cross-section defined in Eq. (2.5). To this end we need to consider the process $p_1 + p_2 = l_1 + l_2 + k$ where k is a final state parton emission as well as $\mathcal{O}(\alpha_s)$ virtual corrections to the Drell-Yan process.

Let us focus first on the real emission contribution. The processes to consider are the emission of a gluon in the Drell-Yan (QCD annihilation) process as well as the contribution of the quark-gluon (QCD Compton) scattering process. Thus we consider the reaction $p_1 + p_2 = l_1 + l_2 + k$ where k is the emitted gluon in the Drell-Yan process and a quark/anti-quark for the Compton process. We need to compute the quantity

$$\begin{aligned} \Sigma^{(1)}(a_T, M^2) &= \int_0^1 dx_1 \int_0^1 dx_2 \left\{ [f_q(x_1) f_{\bar{q}}(x_2) + q \leftrightarrow \bar{q}] \hat{\Sigma}_A^{(1)}(a_T) \right. \\ &\quad \left. + [(f_q(x_1) + f_{\bar{q}}(x_1)) f_g(x_2) + q, \bar{q} \leftrightarrow g] \hat{\Sigma}_C^{(1)}(a_T) \right\} , \end{aligned} \quad (2.22)$$

⁷We can straightforwardly adapt the calculation to include the experimental acceptance cuts when available.

where the partonic quantities $\hat{\Sigma}_{A/C}^{(1)}$ which give the $\mathcal{O}(\alpha_s)$ contribution read

$$\hat{\Sigma}_i^{(1)}(a_T, M^2) = \int d\Phi(l_1, l_2, k) \mathcal{M}_i^2(l_1, l_2, k) \delta(M^2 - 2l_1 \cdot l_2) \Theta(a_T - k_t |\sin \phi|), \quad (2.23)$$

where the index i runs over the contributing subprocesses at this order, i.e. $i = A/C$ denotes the annihilation (Drell-Yan)/Compton subprocesses while \mathcal{M}_i^2 is the appropriate squared matrix element. We have introduced a delta function constraint that indicates we are working at fixed invariant mass of the lepton pair $2l_1 \cdot l_2 = M^2$. Additionally in order to compute the integrated a_T cross-section Eq. (2.5), we need to restrict the additional parton emission k such that we are studying events below some value of a_T . Recalling, from the previous section, that the value of this quantity generated by a gluon with transverse momentum k_t and angle with the lepton axis ϕ is $k_t |\sin \phi|$ we arrive at the step function in the above equation.⁸ We then fold the parton level result with parton distribution functions precisely as for the Born level result Σ_0 reported above.

2.6.1 LO matrix elements

The matrix element squared for the QCD annihilation process from Ref. [33] is (in four dimensions)

$$\begin{aligned} \mathcal{M}_A^2(l_1, l_2, k) = & -16 g^2 \mathcal{G} \frac{C_F}{N_c} M^2 \times \\ & \times \left\{ A_l A_q \left[\left(1 + \frac{\hat{s} - 2t_1 - M^2}{\hat{t}} - \frac{t_1^2 + t_2^2 + \hat{s}(t_1 + t_2 + M^2)}{\hat{t}\hat{u}} \right) + (\hat{u} \leftrightarrow \hat{t}, t_1 \leftrightarrow t_2) \right] \right. \\ & \left. + B_l B_q \left[\left(\frac{(\hat{s} + 2t_1 + M^2)}{\hat{t}} + \frac{\hat{s}(t_1 - t_2)}{\hat{t}\hat{u}} \right) - (\hat{u} \leftrightarrow \hat{t}, t_1 \leftrightarrow t_2) \right] \right\}, \quad (2.24) \end{aligned}$$

⁸As we stated previously this approximation is sufficient up to terms that vanish as $a_T \rightarrow 0$, which we do not compute here.

while for the QCD Compton process, if p_2 represents an incoming gluon, one has

$$\begin{aligned} \mathcal{M}_C^2(l_1, l_2, k) &= -16 g^2 \mathcal{G} \frac{T_R}{N_c} M^2 \times \\ &\times \left\{ A_l A_q \left[\frac{\hat{t} - 2(t_1 + M^2)}{\hat{s}} + \frac{\hat{s} + 2(t_1 + t_2)}{\hat{t}} + \frac{2}{\hat{s}\hat{t}} \left((t_1 + t_2 + M^2)^2 + t_1^2 - t_2 M^2 \right) \right] \right. \\ &\quad \left. + B_l B_q \left[\frac{2(t_1 + M^2) - \hat{t}}{\hat{s}} + \frac{\hat{s} + 2(t_1 + t_2)}{\hat{t}} - \frac{2M^2(2t_1 + t_2 + M^2)}{\hat{s}\hat{t}} \right] \right\}, \quad (2.25) \end{aligned}$$

where we corrected small errors (after an independent recomputation of the above) of an apparent typographical nature in the $B_l B_q$ piece of the annihilation result.

The kinematical variables \hat{u} and \hat{t} are the usual Mandelstam invariants

$$\hat{u} = -2p_1 \cdot k = -\sqrt{s} x_1 k_t e^{-y_k}, \quad \hat{t} = -2p_2 \cdot k = -\sqrt{s} x_2 k_t e^{y_k}, \quad (2.26)$$

where we have explicitly parameterised the momentum k as below

$$k = k_t (\cosh y_k, \cos \phi, \sin \phi, \sinh y_k), \quad (2.27)$$

the parameterisation of the other particles four-momenta being as in the Born case Eq. (2.12).

In the limit of small rescaled transverse momentum $\Delta = k_t^2/M^2$ both matrix elements become collinear singular. In the annihilation subprocess this occurs when the emitted gluon k is collinear to either p_1 (corresponding to $\hat{u} \rightarrow 0$) or p_2 ($\hat{t} \rightarrow 0$). The singularity for $\hat{u} \rightarrow 0$ occurs at positive gluon rapidity y_k , correspondingly the one for $\hat{t} \rightarrow 0$ occurs at negative y_k . The matrix element for the Compton process shows only a collinear divergence when an outgoing quark is collinear to the incoming gluon, corresponding to $\hat{t} \rightarrow 0$.

In the following we compute the approximated expression of \mathcal{M}_A^2 and \mathcal{M}_C^2 in the collinear limit $\hat{t} \rightarrow 0$. The remaining collinear limit $\hat{u} \rightarrow 0$ of \mathcal{M}_A^2 gives an identical result after integration over the lepton rapidity. Neglecting terms of

relative order k_t one has

$$\begin{aligned}
l_T &\simeq \frac{M^2}{\sqrt{s}(x_1 e^{-y} + z x_2 e^y)}, & \hat{t} &\simeq -\frac{k_t^2}{1-z}, & \hat{u} &\simeq -\frac{1-z}{z} M^2, \\
t_1 &\simeq -\frac{x_1 e^{-y} M^2}{(x_1 e^{-y} + z x_2 e^y)}, & t_2 &\simeq -\frac{x_2 e^y M^2}{(x_1 e^{-y} + z x_2 e^y)}, & M^2 &\simeq -(t_1 + z t_2),
\end{aligned} \tag{2.28}$$

where $1-z$ is the fraction of the parent partons energy carried off by the radiated parton. Substituting these expressions in Eq. (2.24) and Eq. (2.25) one obtains

$$\mathcal{M}_A^2(l_1, l_2, k) \simeq \frac{16 g^2}{z k_t^2} \mathcal{G} \frac{C_F}{N_c} (1+z^2) [A_l A_q (t_1^2 + z^2 t_2^2) + B_l B_q (t_1^2 - z^2 t_2^2)], \tag{2.29}$$

and

$$\mathcal{M}_C^2(l_1, l_2, k) \simeq \frac{16 g^2}{z k_t^2} \mathcal{G} \frac{T_R}{N_c} (1-z) [z^2 + (1-z)^2] [A_l A_q (t_1^2 + z^2 t_2^2) + B_l B_q (t_1^2 - z^2 t_2^2)]. \tag{2.30}$$

where the collinear singularity $1/k_t^2$ has been isolated. Note that the result is proportional to the Born matrix element in Eq. (2.7) with x_2 replaced by $z x_2$, indicating that the momentum fraction of the parton entering the hard scattering has been reduced by a factor z after the emission of a collinear gluon.

2.6.2 Integration over three-body phase-space

We now need to integrate the squared matrix elements over a three-body Lorentz invariant phase-space Φ , since in addition to the final state lepton four-momenta l_1, l_2 we also have a final state emitted parton k .

The Lorentz invariant phase-space is now

$$\int d\Phi(l_1, l_2, k) = \frac{1}{2\hat{s}} \int \frac{d^3 l_1}{2(2\pi)^3 l_{10}} \frac{d^3 l_2}{2(2\pi)^3 l_{20}} \frac{d^3 k}{2(2\pi)^3 k_0} (2\pi)^4 \delta^4(p_1 + p_2 - l_1 - l_2 - k). \tag{2.31}$$

Following the same procedure as in the Born case we perform the trivial integration over l_2 and obtain the leading order QCD correction to the Born result (2.14)

(for the moment we are considering just real emission terms indicated below by the label r)

$$\begin{aligned} \Sigma_r^{(1)}(M^2) &= \sum_{i=A,C} \int_0^1 dx_1 f(x_1) \int_0^1 dx_2 f(x_2) \times \\ &\times \frac{1}{2\hat{s}} \int \frac{l_T dl_T dy}{4\pi} \frac{d^3 k}{2(2\pi)^3 k_0} \delta(M^2 + t_1 + t_2 + 2l_1 \cdot k) \times \\ &\times \delta\left(M^2 - x_1 x_2 s \left(1 - \frac{2p_1 \cdot k}{\hat{s}} - \frac{2p_2 \cdot k}{\hat{s}}\right)\right) \mathcal{M}_i^2. \end{aligned} \quad (2.32)$$

Here the factor $(1 - \frac{2p_1 \cdot k}{\hat{s}} - \frac{2p_2 \cdot k}{\hat{s}})$ accounts for the energy-momentum carried off by the radiated parton k while the index $i = A$ pertains to the QCD annihilation process while $i = C$ indicates the QCD Compton process. Noting that one has as before $t_1 = -\sqrt{s} x_1 l_T e^{-y}$, $t_2 = -\sqrt{s} x_2 l_T e^y$ and additionally $2l_1 \cdot k = 2l_T k_t (\cosh(y - y_k) - \cos \phi)$, we can use the constraint $\delta(M^2 + t_1 + t_2 + 2l_1 \cdot k)$ to integrate over l_T and the value of l_T (and hence t_1, t_2) is thus fixed in terms of other parameters:

$$\begin{aligned} l_T &= \frac{M^2}{\sqrt{s} \left(x_1 e^{-y} + x_2 e^y - 2\frac{k_t}{\sqrt{s}} (\cosh(y - y_k) - \cos \phi)\right)}, \\ t_1 &= -\frac{x_1 e^{-y} M^2}{\left(x_1 e^{-y} + x_2 e^y - 2\frac{k_t}{\sqrt{s}} (\cosh(y - y_k) - \cos \phi)\right)}, \end{aligned} \quad (2.33)$$

with the expression for t_2 the same as that for t_1 except that $x_1 e^{-y}$ in the numerator of the above expression for t_1 is to be replaced by $x_2 e^y$. After integrating away the l_T one gets

$$\begin{aligned} \Sigma_r^{(1)}(M^2) &= \sum_{i=A,C} \int_0^1 dx_1 f(x_1) \int_0^1 dx_2 f(x_2) \frac{1}{8\pi s} \int dy \frac{d^3 k}{2(2\pi)^3 k_0} \times \\ &\times \frac{M^2}{\hat{s} \left(x_1 e^{-y} + x_2 e^y - \frac{2k_t}{\sqrt{s}} (\cosh(y - y_k) - \cos \phi)\right)^2} \mathcal{M}_i^2 \delta(M^2 - z x_1 x_2 s). \end{aligned} \quad (2.34)$$

where we introduced $z = 1 - 2(p_1 \cdot k)/\hat{s} - 2(p_2 \cdot k)/\hat{s}$.

We are now ready to integrate over the parton and lepton phase-space variables. Since we are interested in the specific cross-section in Eq. (2.5), we need to integrate over the phase-space such that the value of the a_T is below some fixed value. Further we are interested in the small a_T logarithmic terms so that we consider the region $a_T/M \ll 1$.

To avoid having to explicitly invoke virtual corrections we shall calculate the cross-section for all events *above* a_T and subtract this from the total $\mathcal{O}(\alpha_s)$ result $\Sigma^{(1)}(M^2)$ which can be taken from the literature [34]:

$$\Sigma^{(1)}(a_T, M^2) = \Sigma^{(1)}(M^2) - \Sigma_c^{(1)}(a_T, M^2), \quad (2.35)$$

where we shall calculate $\Sigma_c^{(1)}(a_T, M^2) = \int_{a_T} \frac{d\sigma}{da'_T dM^2} da'_T$.

Moreover since we are interested in just the soft and/or collinear logarithmic behaviour we can use the form of the a_T in the soft/collinear limit derived in section 2.4. Thus we evaluate the integrals in Eq. (2.34) with the constraint $\Theta(k_t |\sin \phi| - a_T)$. In order to carry out the integration let us express the parton phase-space in terms of rapidity y_k , k_t and ϕ . Thus we have

$$\begin{aligned} \int \frac{d^3 k}{2(2\pi)^3 k_0} &= \int \frac{k_t dk_t dy_k d\phi}{2(2\pi)^3} \\ &= \left(\frac{M^2}{16\pi^2} \right) \int \frac{d\phi}{2\pi} \int dy_k \int \frac{dz d\Delta}{\sqrt{(1-z)^2 - 4z\Delta}} [\delta(y_k - y_+) + \delta(y_k - y_-)], \end{aligned} \quad (2.36)$$

where we used

$$z = 1 - \frac{k_t}{\sqrt{s}x_2} e^{-y_k} - \frac{k_t}{\sqrt{s}x_1} e^{y_k}, \quad (2.37)$$

which follows from the definition of z and where we also introduced the dimensionless variable $\Delta = k_t^2/M^2$. A fixed value of z corresponds to two values of the emitted parton rapidity

$$y_{\pm} = \ln \left[\frac{\sqrt{s}x_1}{2k_t} \left((1-z) \pm \sqrt{(1-z)^2 - 4z\Delta} \right) \right]. \quad (2.38)$$

Having obtained the phase-space in terms of convenient variables we need to write the squared matrix elements in terms of the same. We first analyse the QCD annihilation correction and next the Compton piece. In the annihilation contribution one has singularities due to the vanishing of the invariants \hat{t} and \hat{u} with the $1/(\hat{t}\hat{u})$ piece contributing up to double logarithms due to soft and collinear radiation by either incoming parton and the $1/\hat{t}$ and $1/\hat{u}$ singularities generating single logarithms. The double logarithms arise from low energy and large rapidity emissions (soft and collinear emissions) while the single-logarithms from energetic collinear emissions, hence it is the small k_t limit of the squared matrix elements that generates the relevant logarithmic behaviour. Thus we write the squared matrix element \mathcal{M}_A^2 in Eq. (2.24) in terms of the variables Δ and z and then find the leading small Δ behaviour. Specifically in the $\Delta \rightarrow 0$ limit, considering only the $1/\hat{t}$ singular piece, the factor appearing in (2.34) has the following behaviour (keeping for now only the $A_l A_q$ piece of the matrix element):

$$\frac{1}{\hat{s}} \mathcal{M}_A^2 \frac{M^2}{s \left(x_1 e^{-y} + x_2 e^y - \frac{2k_t}{\sqrt{s}} (\cosh(y - y_k) - \cos \phi) \right)^2} \approx 16 g^2 \mathcal{G} \frac{A_l A_q}{N_c} \frac{C_F}{\Delta} (1 + z^2) \frac{M^2}{s} \frac{x_1^2 e^{-2y} + x_2^2 z^2 e^{2y}}{(x_1 e^{-y} + x_2 z e^y)^4}. \quad (2.39)$$

Performing the integral over all rapidities y of the lepton, the above factor produces $16g^2 \mathcal{G} \frac{A_l A_q}{N_c} \frac{C_F}{\Delta} \frac{1+z^2}{3}$. The corresponding $B_l B_q$ piece of the squared matrix element vanishes upon integration over all rapidities.

Since the $1/\hat{u}$ singular term, after integration over all lepton rapidities, gives us the same result as that arising from Eq. (2.39), we can write for the annihilation

process (using eqs. (2.34), (2.36)) and $g^2 = 4\pi\alpha_s$

$$\begin{aligned} \Sigma_{A,c}^{(1)} = \mathcal{G} \frac{A_l A_q}{N_c} \int dx_1 dx_2 f(x_1) f(x_2) \frac{M^2}{3\pi} \int dz \delta(M^2 - x_1 x_2 z s) \\ \int \frac{d\phi}{2\pi} C_F \frac{\alpha_s}{2\pi} \frac{2(1+z^2)}{\sqrt{(1-z)^2 - 4z\Delta}} \frac{d\Delta}{\Delta} \Theta\left(\sqrt{\Delta} |\sin \phi| - \frac{a_T}{M}\right). \end{aligned} \quad (2.40)$$

Following the same procedure for the Compton process one finds instead

$$\begin{aligned} \frac{1}{\hat{s}} \mathcal{M}_C^2 \frac{M^2}{s \left(x_1 e^{-y} + x_2 e^y - \frac{2k_t}{\sqrt{s}} (\cosh(y - y_k) - \cos \phi)\right)^2} \\ \approx 16 g^2 \mathcal{G} \frac{A_l A_q}{N_c} \frac{T_R}{\Delta} (1-z) [z^2 + (1-z)^2] \frac{M^2}{s} \frac{x_1^2 e^{-2y} + x_2^2 z^2 e^{2y}}{(x_1 e^{-y} + x_2 z e^y)^4}, \end{aligned} \quad (2.41)$$

which after integration over the rapidity y reduces to $16g^2 \mathcal{G} \frac{A_l A_q}{N_c} \frac{T_R}{\Delta} (1-z) \frac{z^2 + (1-z)^2}{3}$.

Thus we have for this piece

$$\begin{aligned} \Sigma_{C,c}^{(1)} = \mathcal{G} \frac{A_l A_q}{N_c} \int dx_1 dx_2 f(x_1) f(x_2) \frac{M^2}{3\pi} \int dz \delta(M^2 - x_1 x_2 z s) \\ \int \frac{d\phi}{2\pi} T_R \frac{\alpha_s}{2\pi} \frac{(1+z) [z^2 + (1-z)^2]}{\sqrt{(1-z)^2 - 4z\Delta}} \frac{d\Delta}{\Delta} \Theta\left(\sqrt{\Delta} |\sin \phi| - \frac{a_T}{M}\right). \end{aligned} \quad (2.42)$$

Therefore, accounting for virtual corrections and retaining only singular terms in the limit $k_t \rightarrow 0$ (which are the source of logarithms in a_T), we arrive at the result for the annihilation contribution

$$\begin{aligned} \Sigma_A^{(1)}(a_T, M^2) = -\mathcal{G} \frac{M^2}{3\pi} \frac{A_l A_q}{N_c} \int_0^1 dx_1 \int_0^1 dx_2 \int_0^1 dz [f_q(x_1) f_{\bar{q}}(x_2) + q \leftrightarrow \bar{q}] \times \\ \times \delta(M^2 - s x_1 x_2 z) \int_0^{2\pi} \frac{d\phi}{2\pi} \int_0^1 \frac{d\Delta}{\Delta} C_F \frac{\alpha_s}{2\pi} \frac{2(1+z^2)}{\sqrt{(1-z)^2 - 4z\Delta}} \Theta\left(\sqrt{\Delta} |\sin \phi| - \frac{a_T}{M}\right), \end{aligned} \quad (2.43)$$

while that for the Compton subprocess reads

$$\begin{aligned} \Sigma_C^{(1)}(a_T, M^2) = & -\mathcal{G} \frac{M^2}{3\pi} \frac{A_l A_q}{N_c} \int_0^1 dx_1 \int_0^1 dx_2 \int_0^1 dz [(f_q(x_1) + f_{\bar{q}}(x_1)) f_g(x_2) + q, \bar{q} \leftrightarrow g] \times \\ & \times \delta(M^2 - s x_1 x_2 z) \int_0^{2\pi} \frac{d\phi}{2\pi} \int_0^1 \frac{d\Delta}{\Delta} T_R \frac{\alpha_s}{2\pi} \frac{(1-z)[z^2 + (1-z)^2]}{\sqrt{(1-z)^2 - 4z\Delta}} \Theta\left(\sqrt{\Delta} |\sin \phi| - \frac{a_T}{M}\right). \end{aligned} \quad (2.44)$$

Note that the above equations involve the step function constraint $\Theta(k_t |\sin \phi| - a_T)$ which represents the fact that the number of events with $k_t |\sin \phi| < a_T$ is equal to the total rate minus the events with $k_t |\sin \phi| > a_T$. Since the total rate is a number independent of a_T , we can simply compute the events with $k_t |\sin \phi| > a_T$ to obtain the logarithmic a_T dependence, which is what we have done above.

In the above equations we have also parametrised the integral over the emitted parton momentum via the rescaled transverse momentum $\Delta = k_t^2/M^2$, the azimuthal angle ϕ and z where in the collinear limit $1 - z$ is just the fraction of the parent partons energy carried off by the radiated gluon.

2.6.3 Logarithmic singularities in the a_T distribution

The above results are sufficient to obtain the logarithmic structure in a_T and compare it to the corresponding result for the Z boson p_T distribution. In this respect we note that the only difference between the results reported immediately above and those for the p_T case are the $|\sin \phi|$ terms in the step function constraints above. While at the leading order these will essentially just be a matter of detail we shall see that the $\sin \phi$ dependence has an important role to play in the shape of the resummed spectrum.

To complete the calculations one proceeds as in the Z boson p_T case and hence we take the moments with respect to the standard Drell-Yan variable $\tau = \frac{M^2}{s}$,

thereby defining

$$\tilde{\Sigma}(N, a_T) = \int_0^1 d\tau \tau^{N-1} \Sigma(a_T, M^2), \quad (2.45)$$

which can be expressed as a sum over the moment space annihilation and Compton terms $\tilde{\Sigma}(N, a_T) = \tilde{\Sigma}_A(N, a_T) + \tilde{\Sigma}_C(N, a_T)$.

The Born level Drell-Yan contribution can then be expressed in moment space as

$$\tilde{\Sigma}^{(0)}(N) = \frac{\mathcal{G}}{3\pi} \frac{A_l A_q}{N_c} F_A(N), \quad (2.46)$$

where $F_A(N)$ denotes the moment integrals of the parton distribution functions

$$\begin{aligned} F_A(N) &= \int_0^1 dx_1 x_1^N \int_0^1 dx_2 x_2^N [f_q(x_1) f_{\bar{q}}(x_2) + q \leftrightarrow \bar{q}] \\ &= \tilde{f}_q(N) \tilde{f}_{\bar{q}}(N) + q \leftrightarrow \bar{q}, \end{aligned} \quad (2.47)$$

where we introduced $\tilde{f}(N)$, the moments of the parton distributions.

Likewise the $\mathcal{O}(\alpha_s)$ annihilation contribution can be expressed as

$$\begin{aligned} \tilde{\Sigma}_A^{(1)}(N, a_T) &= -\frac{\mathcal{G}}{3\pi} \frac{A_l A_q}{N_c} F_A(N) \int dz z^N \int_0^{2\pi} \frac{d\phi}{2\pi} \times \\ &\quad \times \int_0^1 \frac{d\Delta}{\Delta} C_F \frac{\alpha_s}{2\pi} \frac{2(1+z^2)}{\sqrt{(1-z)^2 - 4z\Delta}} \Theta\left(\sqrt{\Delta} |\sin \phi| - \epsilon\right), \end{aligned} \quad (2.48)$$

where $\epsilon = a_T/M$ is a dimensionless version of the a_T variable.

Performing the integrals over z and Δ we obtain the result

$$\begin{aligned} \tilde{\Sigma}_A^{(1)}(N, a_T) &= -\tilde{\Sigma}^{(0)}(N) \left[2 \frac{\alpha_s}{\pi} \gamma_{qq}(N) \int_0^{2\pi} \frac{d\phi}{2\pi} \ln \frac{|\sin \phi|}{\epsilon} \right. \\ &\quad \left. + \frac{2C_F \alpha_s}{\pi} \int_0^{2\pi} \frac{d\phi}{2\pi} \left(\ln^2 \frac{|\sin \phi|}{\epsilon} - \frac{3}{2} \ln \frac{|\sin \phi|}{\epsilon} \right) \right]. \end{aligned} \quad (2.49)$$

where we introduced the quark anomalous dimension

$$\gamma_{qq}(N) = C_F \int_0^1 dz (z^N - 1) \frac{1+z^2}{1-z}. \quad (2.50)$$

Notice the proportionality of the above result to the Born level result; it is a consequence of the factorization that is valid for logarithmic terms of collinear origin.

We have not integrated over the variable ϕ as yet in order to make the link to results for the p_T distribution. To obtain the $\mathcal{O}(\alpha_s)$ integrated cross-section for the p_T case the same formulae as reported above apply but one replaces $|\sin \phi|$ by unity while ϵ would denote p_T/M . The ϕ integral is then trivial and can be replaced by unity. For the a_T variable on performing the ϕ integral we use the results

$$\int_0^{2\pi} \frac{d\phi}{2\pi} \ln^2 |\sin \phi| = \ln^2 2 + \frac{\pi^2}{12}, \quad (2.51)$$

$$\int_0^{2\pi} \frac{d\phi}{2\pi} \ln |\sin \phi| = -\ln 2, \quad (2.52)$$

to obtain

$$\begin{aligned} \tilde{\Sigma}_A^{(1)}(N, a_T) &= -\tilde{\Sigma}^{(0)}(N) \times \\ &\times \left[2 \frac{\alpha_s}{\pi} \gamma_{qq}(N) \ln \frac{1}{2\epsilon} + \frac{2C_F \alpha_s}{\pi} \left(\ln^2 \frac{1}{2\epsilon} - \frac{3}{2} \ln \frac{1}{2\epsilon} \right) + \frac{C_F \alpha_s \pi^2}{2\pi \cdot 3} \right]. \end{aligned} \quad (2.53)$$

The corresponding result for the QCD Compton process is purely single logarithmic and reads

$$\begin{aligned} \tilde{\Sigma}_C^{(1)}(N, a_T) &= -\frac{\mathcal{G}}{3\pi} \frac{A_l A_q}{N_c} F_C(N) \left(2 \frac{\alpha_s}{\pi} \gamma_{qg}(N) \int_0^{2\pi} \frac{d\phi}{2\pi} \ln \frac{|\sin \phi|}{\epsilon} \right) \\ &= -\frac{\mathcal{G}}{3\pi} \frac{A_l A_q}{N_c} F_C(N) 2 \frac{\alpha_s}{\pi} \gamma_{qg}(N) \ln \frac{1}{2\epsilon}, \end{aligned} \quad (2.54)$$

where

$$\gamma_{qg}(N) = T_R \int_0^1 dz z^N [z^2 + (1-z)^2], \quad (2.55)$$

and $F_C(N)$ is the moment integral of the relevant combination of parton density

functions

$$\begin{aligned}
F_C(N) &= \int_0^1 dx_1 x_1^N \int_0^1 dx_2 x_2^N [(f_q(x_1) + f_{\bar{q}}(x_1)) f_g(x_2) + q, \bar{q} \leftrightarrow g] \\
&= \left(\tilde{f}_q(N) + \tilde{f}_{\bar{q}}(N) \right) \tilde{f}_g(N) + q, \bar{q} \leftrightarrow g.
\end{aligned} \tag{2.56}$$

In our final results, eqs. (2.53) and (2.54), we have neglected constant terms that are identical to those for the Drell-Yan p_T distribution computed for instance in [35].

We note that the logarithms found here, both in the Drell-Yan and Compton contributions, are the same as those for the p_T variable with the replacement $\epsilon \rightarrow 2\epsilon$. In other words as far as the logarithmic dependence is concerned we obtain that the result for the cross-section for events with $a_T < \epsilon M$ is the same as the result for the variable $p_T/2 < \epsilon M$. The only other effect, at this order, of the $|\sin \phi|$ term is to generate a constant term $\frac{C_F \alpha_s \pi^2}{2\pi} \frac{\pi^2}{3}$ reported above. Thus to leading order in α_s we have simply

$$\Sigma^{(1)}(a_T, M^2)|_{a_T=\epsilon M} - \Sigma^{(1)}\left(\frac{p_T}{2}\right)|_{p_T/2=\epsilon M} = -\Sigma^{(0)} C_F \frac{\alpha_s \pi^2}{2\pi} \frac{\pi^2}{3}. \tag{2.57}$$

In writing the above we have returned to τ space by inverting the Mellin transform so as to obtain the result in terms of the factor $\Sigma^{(0)}$ rather than $\tilde{\Sigma}^{(0)}(N)$.

The result above has been verified by using a fixed-order program such as MCFM. One can obtain the results for the integrated cross-sections for a_T and $p_T/2$ and the difference between them should be a constant with the value reported above. This is indeed the case, as one can see from the plot in figure 2.4, where the difference in Eq. (2.57) generated using the numerical fixed-order program MCFM [31], divided by the Born cross section $\Sigma^{(0)}$, is plotted against $L = \ln(\epsilon)$. The results from MCFM agree with our expectation (2.57). In order to show the smoothest curve we have taken the case where the Z decay has been treated fully inclusively (i.e

we have not placed rapidity cuts) and a narrow width approximation eventually employed but we have checked our results agree with MCFM for arbitrary cuts on lepton rapidities.

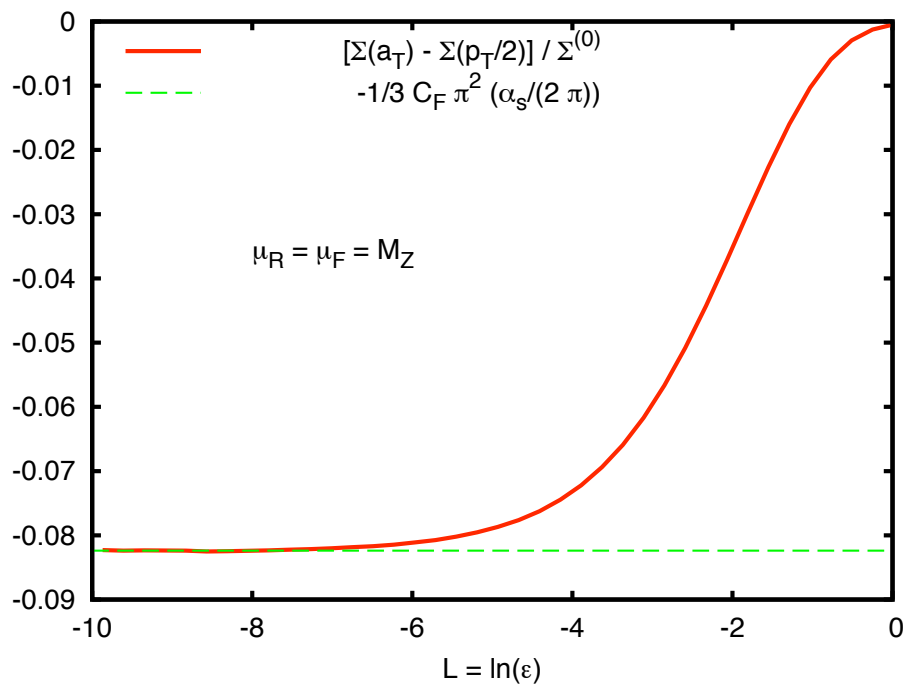


Figure 2.4: The difference between the integrated distributions for a_T and $p_T/2$. Here we have used the CTEQ6M pdf set [36] and both factorisation and renormalisation scales μ_F and μ_R have been fixed at the Z boson mass M_Z . The statistical errors of the Monte Carlo are small compared to the width of the curve and the number of bins in L are large enough to make the plot look like a continuous curve.

Having carried out the fixed-order computation, which serves to illustrate some important points, we shall shift our attention to the resummation of logarithms to all orders.

2.7 Resummation of large logarithms in a_T

In the present section we address the issue of resummation for the a_T variable. We point out that there are some similarities to resummation for the p_T distribution but also some important differences that manifest themselves in the shape of the resummed distribution. We aim to provide a next-to-leading logarithmic (NLL) resummation that we envisage could be extended to NNLL level subsequently. The NLL resummed form we provide here can however already be used after matching to full next-to-leading order (NLO) results for accurate phenomenological studies of a_T .

We shall carry out the resummation of the large logarithms in the ratio of two scales M and a_T which become disparate at small a_T , $a_T \ll M$. We already derived the dependence of the a_T on multiple soft and/or collinear emissions in the preceding section and hence in order to carry out the resummation we next need to address the dynamics of multiple low k_t emissions. We shall first treat only the Drell-Yan process and later specify the role of the QCD Compton production process.

We shall study as before the integrated cross-section representing the number of events below some fixed value of a_T , defined in Eq. (2.5), from which one can obtain the a_T distribution by differentiating with respect to a_T . Also as we emphasised in the previous section we are working at fixed invariant mass of the lepton pair purely as an illustrative example and we can straightforwardly adapt our calculations to take into account experimental cuts on for instance lepton rapidities, which in any case do not affect the resummation.

We consider again the incoming partons as carrying momentum fractions x_1 and x_2 of the incoming hadrons which means that at Born level where they annihilate

to form the lepton pair via virtual Z production we have simply $M^2 = \hat{s} = sx_1x_2$, where the Mandelstam invariant \hat{s} denotes the partonic centre of mass energy. Beyond the Born level one has to take account of gluon radiation and to this end we introduce as in the previous section the quantity $z = M^2/\hat{s}$ such that $1 - z$ represents the fractional energy loss of the incoming partons due to the radiation of collinear gluons. Thus in the limit $z \rightarrow 1$ one is probing soft and collinear radiation while away from $z = 1$ we will be dealing with energetic collinear emission. We note here that for the purpose of generating the logarithms we resum we do not have to examine large-angle radiation and the collinear limit is sufficient as for the usual p_T distribution. In fact since the a_T resummation we aim to carry out shares several common features with the well-known p_T distribution we shall only sketch the resummation concentrating instead on features of the a_T which lead to differences from the p_T variable. For a recent detailed justification of the approximations that lead to NLL resummation for the p_T case as well as for other variables the reader is referred to Ref. [37].

We work in the centre-of-mass frame of the colliding partons and in moment space where we take moments with respect to $\tau = M^2/s$ of the cross-section in Eq. (2.5) as in the fixed-order calculations we carried out. Taking moments enables us to write for the emission of multiple collinear and optionally soft gluons

$$\tilde{\Sigma}(N, a_T) = \tilde{\Sigma}^{(0)}(N) W_N(a_T), \quad (2.58)$$

where $\tilde{\Sigma}^{(0)}(N)$ is the Born level result in Eq. (2.46). The effects of multiple collinear (and optionally soft) gluon emission from the incoming projectiles are included in the function W_N which can be expressed to next-to-leading logarithmic (NLL) in

the standard factorised form

$$W_N^{\text{real}}(a_T) = \sum_{n=0}^{\infty} \frac{1}{n!} \prod_{i=1}^n \int dz_i \frac{dk_{ti}^2}{k_{ti}^2} \frac{d\phi_i}{2\pi} \times \\ \times z_i^N 2C_F \frac{\alpha_s(k_{ti}^2)}{2\pi} \left(\frac{1+z_i^2}{1-z_i} \right) \Theta \left(a_T - \left| \sum_i v(k_i) \right| \right), \quad (2.59)$$

where $1 - z_i$ denotes the fraction of momentum carried away by emission of a quasi-collinear gluon i from the incoming hard projectile so that $M^2/\hat{s} = z = \prod_i z_i$ and k_{ti} is the transverse momentum of gluon i with respect to the hard emitting incoming partons.

In writing the above results we have used an independent emission approximation, valid to NLL accuracy, where the emission probability for n collinear gluons is merely the product of single gluon emission probabilities, which factorise from the Born level production of the hard lepton pair.⁹ The single gluon emission probability to the same NLL accuracy is given by the leading order splitting function for the splitting of a quark to a quasi-collinear quark and gluon (weighted by the running strong coupling),

$$P_{qq}(z) \frac{\alpha_s(k_t^2)}{2\pi} = C_F \frac{\alpha_s(k_t^2)}{2\pi} \frac{1+z^2}{1-z}, \quad (2.60)$$

with α_s defined in the CMW scheme [40]. We have inserted a factor of two to take account of the fact that there are two hard incoming partons which independently emit collinear gluons. We have also taken care of the constraint on real gluon emission, imposed by the requirement that the sum of the components of the k_{ti} normal to the axis in Eq. (2.1) (denoted by $v(k_i) = k_{ti} \sin \phi_i$) is less than a_T . We have integrated over the leptons, holding the invariant mass M fixed, and taken

⁹This approximation is invalid for situations when one is examining soft radiation in a limited angular interval away from hard emitting particles [38,39], which is not the case here.

moments to obtain the full zeroth order Drell-Yan result $\tilde{\Sigma}^{(0)}(N)$, which multiplies the function W_N containing all-order radiative effects.

All of the above arguments would also apply to the case of the p_T variable. Thus while the dynamics of multiple soft/collinear emission is treated exactly as for the p_T resummation the difference between the p_T and our resummation arises purely due to the different form of the argument of the step function restricting multiple real emission. Thus while for the p_T variable the phase space constraint involves a two-dimensional vector sum $\Theta\left(p_T - |\sum_i \vec{k}_{ti}|\right)$, in the present case we have a one dimensional sum of the components of the gluon k_t normal to the lepton thrust axis, $v(k_i) = k_{ti} \sin \phi_i$. One encounters such a one dimensional sum also in cases such as azimuthal correlations in DIS [30,41] and the resummation of the p_t difference between jets in dijet production [32]. It is this difference that will be responsible for different features of the a_T distribution as we shall further clarify below. The relationship between azimuthal correlations and the a_T is no surprise since the a_T variable is proportional to $\pi - \Delta\phi_u$, the deviation of the azimuthal interval between the leptons from its Born value π .

In order to further simplify Eq. (2.59) we also factorise the phase space constraint using a Fourier representation of the step function [41]

$$\Theta\left(a_T - \left|\sum_i v(k_i)\right|\right) = \frac{1}{\pi} \int_{-\infty}^{\infty} \frac{db}{b} \sin(ba_T) \prod_i e^{ibv(k_i)}. \quad (2.61)$$

Note the presence of the $\sin(ba_T)$ function which is a consequence of addressing a one dimensional sum as opposed to the Bessel function J_1 one encounters in resummation of the p_T cross-section. With both the multiple emission probability and phase space factorised as above it is easy to carry out the infinite sum in

Eq. (2.59) which yields

$$W_N^{\text{real}}(a_T) = \frac{1}{\pi} \int_{-\infty}^{\infty} \frac{db}{b} \sin(ba_T) e^{R^{\text{real}}(b)}, \quad (2.62)$$

with the exponentiated real gluon emission contribution

$$R^{\text{real}}(b) = \int dz \frac{dk_t^2}{k_t^2} \frac{d\phi}{2\pi} z^N 2C_F \frac{\alpha_s(k_t^2)}{2\pi} \left(\frac{1+z^2}{1-z} \right) e^{ibv(k)} \Theta \left(1 - z - \frac{k_t}{M} \right). \quad (2.63)$$

The kinematic limit on the z integration is set in such a way that one correctly accounts for soft large angle emissions.

Next we include all-order virtual corrections which straightforwardly exponentiate in the soft-collinear limit to yield finally

$$W_N(a_T) = \frac{2}{\pi} \int_0^\infty \frac{db}{b} \sin(ba_T) e^{-R(b)}, \quad (2.64)$$

where

$$\begin{aligned} -R(b) = R^{\text{real}} + R^{\text{virtual}} &= \int dz \frac{dk_t^2}{k_t^2} \frac{d\phi}{2\pi} 2C_F \frac{\alpha_s(k_t^2)}{2\pi} \left(\frac{1+z^2}{1-z} \right) \times \\ &\times (z^N e^{ibv(k)} - 1) \Theta \left(1 - z - \frac{k_t}{M} \right), \end{aligned} \quad (2.65)$$

where it should be clear that the term corresponding to the -1 added to the real contribution $z^N e^{ibv(k)}$ corresponds to the virtual corrections. Note that the virtual corrections are naturally independent of both Fourier and Mellin variables b and N respectively since they do not change the longitudinal or transverse momentum of the incoming partons and hence exponentiate directly. We are thus left to analyse $R(b)$ the ‘‘radiator’’ up to single-logarithmic accuracy.

2.7.1 The resummed exponent

Here we shall evaluate the function $R(b)$ representing the resummed exponent to the required accuracy. We shall first explicitly introduce a factorisation scale Q_0^2

to render the integrals over k_t finite. Later we will be able to take the $Q_0 \rightarrow 0$ limit. Thus one considers all emissions with transverse momenta below Q_0 to be included in the pdfs which are defined at scale Q_0 such that the factor $\tilde{\Sigma}^{(0)}(N)$ reads

$$\tilde{\Sigma}^{(0)}(N) = \frac{A_l A_q}{N_c} \frac{\mathcal{G}}{3\pi} F_A(N, Q_0^2), \quad (2.66)$$

with

$$\begin{aligned} F_A(N, Q_0^2) &= \int_0^1 dx_1 x_1^N \int_0^1 dx_2 x_2^N [f_q(x_1, Q_0^2) f_{\bar{q}}(x_2, Q_0^2) + q \leftrightarrow \bar{q}] \\ &= \left[\tilde{f}_q(N, Q_0^2) \tilde{f}_{\bar{q}}(N, Q_0^2) + q \leftrightarrow \bar{q} \right]. \end{aligned} \quad (2.67)$$

Thus while in the fixed-order calculation of the previous section the pdfs could be treated as bare scale independent quantities, for the resummed calculation we start with full pdfs evaluated at an arbitrary (perturbative) factorisation scale. The k_t integration in the perturbative radiator should now be performed with scale $k_t > Q_0$. We next follow the method of Ref. [42] where an essentially identical integral was performed for the radiator.

First, following the method of Ref. [42] we change the argument of the pdfs from Q_0 to the correct hard scale of the problem, the pair invariant mass M , via DGLAP evolution. To be precise we use for the quark distribution

$$\tilde{f}_q(N, Q_0^2) = \tilde{f}_q(N, M^2) e^{-\int_{Q_0^2}^{M^2} \frac{dk_t^2}{k_t^2} \frac{\alpha_s(k_t^2)}{2\pi} \gamma_{qq}(N)}, \quad (2.68)$$

and likewise for the anti-quark distribution where $\gamma_{qq}(N)$ is the standard quark anomalous dimension matrix. Note that we have not yet considered the QCD Compton scattering process and the corresponding evolution of the quark pdf from incoming gluons via the γ_{qg} anomalous dimension matrix, which we shall include in the final result by using the full pdf evolution rather than the simplified form reported immediately above. Carrying out the above step results in a modified

radiator such that one now has

$$R(b) = 2C_F \int_{Q_0^2}^{M^2} \frac{dk_t^2}{k_t^2} \frac{\alpha_s(k_t^2)}{2\pi} \int_0^{2\pi} \frac{d\phi}{2\pi} \times \\ \times \left[\int_0^1 dz \frac{1+z^2}{1-z} (1 - z^N e^{ibv(k)}) \Theta \left(1 - z - \frac{k_t}{M} \right) + \frac{\gamma_{qq}(N)}{C_F} \right]. \quad (2.69)$$

Using the definition of the anomalous dimension $\gamma_{qq}(N)$ we can write the above (see for instance Ref. [42]) as

$$R(b) = 2C_F \int_{Q_0^2}^{M^2} \frac{dk_t^2}{k_t^2} \frac{\alpha_s(k_t^2)}{2\pi} \int_0^{2\pi} \frac{d\phi}{2\pi} \int_0^1 dz z^N \frac{1+z^2}{1-z} (1 - e^{ibv(k)}) \Theta \left(1 - z - \frac{k_t}{M} \right), \quad (2.70)$$

where in arriving at the last equation we neglected terms of $\mathcal{O}(k_t/M)$.

To NLL accuracy we can further make the approximation [41]

$$1 - e^{ibv(k)} \rightarrow \Theta \left(k_t |\sin \phi| - \frac{1}{\bar{b}} \right), \quad (2.71)$$

where we used the fact that in the present case $v(k_i) = k_t \sin \phi_i$ with $\bar{b} = b e^{\gamma_E}$.

Thus one gets for the radiator $R(b) \equiv R(\bar{b})$

$$R(\bar{b}) = 2C_F \int_{Q_0^2}^{M^2} \frac{dk_t^2}{k_t^2} \frac{\alpha_s(k_t^2)}{2\pi} \int_0^{2\pi} \frac{d\phi}{2\pi} \int_0^1 dz z^N \frac{1+z^2}{1-z} \times \\ \times \Theta \left(k_t |\sin \phi| - \frac{1}{\bar{b}} \right) \Theta \left(1 - z - \frac{k_t}{M} \right). \quad (2.72)$$

We now evaluate the radiator to the required accuracy. Performing the z integration to NLL accuracy, and neglecting terms of relative order k_t/M , one arrives at

$$R(\bar{b}) = 2C_F \int_0^{2\pi} \frac{d\phi}{2\pi} \int_0^{M^2} \frac{dk_t^2}{k_t^2} \frac{\alpha_s(k_t^2)}{2\pi} \Theta \left(k_t |\sin \phi| - \frac{1}{\bar{b}} \right) \left(\ln \frac{M^2}{k_t^2} - \frac{3}{2} + \frac{\gamma_{qq}(N)}{C_F} \right), \quad (2.73)$$

where in the last line we took $Q_0 \rightarrow 0$ since the k_t integral is now cut-off by the step function $\Theta [k_t |\sin \phi| - 1/\bar{b}]$ and chose to perform the ϕ integration at the end.

We note that the only difference between the radiator above and the standard p_T distribution is the factor $|\sin \phi|$ multiplying k_t in the step function condition above. This will result in an additional single-logarithmic contribution not present in the p_T resummation results.

In order to deal with the ϕ dependence to NLL accuracy we expand (as in Ref. [32]) Eq. (2.73) about $|\sin \phi| = 1$ in powers of $\ln |\sin \phi|$ to obtain

$$R(\bar{b}) = 2C_F \int_0^{M^2} \frac{dk_t^2}{k_t^2} \frac{\alpha_s(k_t^2)}{2\pi} \Theta \left(k_t - \frac{1}{\bar{b}} \right) \left(\ln \frac{M^2}{k_t^2} - \frac{3}{2} + \frac{\gamma_{qq}(N)}{C_F} \right) + \frac{\partial R(\bar{b})}{\partial \ln(\bar{b}M)} \int_0^{2\pi} \frac{d\phi}{2\pi} \ln |\sin \phi| + \dots \quad (2.74)$$

where we have neglected higher derivatives of R as they will contribute only beyond NLL accuracy. Moreover in evaluating $\partial R(\bar{b})/\partial \ln(\bar{b}M)$ we can replace R by its leading logarithmic form $R_{\text{LL}}(\bar{b})$ since logarithmic derivatives of any next-to-leading logarithmic pieces of $R(\bar{b})$ will give only NNLL terms that are beyond our accuracy. The first term on the RHS of the above equation is in fact just the radiator we would get for resummation of the Z boson p_T distribution which contains both leading and next-to-leading logarithmic terms. The second term on the RHS accounts for the ϕ dependence of the problem and is purely next-to-leading logarithmic in nature since it contains the logarithmic derivative of $R_{\text{LL}}(\bar{b})$. Thus we need to evaluate the first term on the RHS of Eq. (2.73) and then isolate its leading-logarithmic piece to compute the second term on the RHS.

We carry out the integral over k_t to NLL accuracy using standard techniques [43], i.e. we change the coupling from the CMW to the $\overline{\text{MS}}$ scheme

$$\alpha_s^{\text{CMW}}(k_t^2) = \alpha_s^{\overline{\text{MS}}}(k_t^2) \left(1 + K \frac{\alpha_s^{\overline{\text{MS}}}(k_t^2)}{2\pi} \right), \quad K = C_A \left(\frac{67}{18} - \frac{\pi^2}{6} \right) - \frac{5}{9} n_f, \quad (2.75)$$

and use a two-loop running coupling

$$\alpha_s(k_t^2) = \frac{\alpha_s(M^2)}{1 - \rho} \left[1 - \alpha_s(M^2) \frac{\beta_1 \ln(1 - \rho)}{\beta_0} \right], \quad \rho = \alpha_s(M^2) \beta_0 \ln \frac{M^2}{k_t^2}, \quad (2.76)$$

where $\alpha_s(M^2)$ is a shorthand for $\alpha_s^{\overline{\text{MS}}}(M^2)$. We then obtain the usual expression

$$R(\bar{b}) = L g_1(\alpha_s L) + g_2(\alpha_s L), \quad (2.77)$$

with $L \equiv \ln(\bar{b}^2 M^2)$. The functions g_1 and g_2 are then the leading and next-to-leading logarithmic functions which have the following detailed form

$$\begin{aligned} g_1(\lambda) &= \frac{C_F}{\pi \beta_0 \lambda} [-\lambda - \ln(1 - \lambda)], \quad (2.78) \\ g_2(\lambda) &= \frac{3C_F}{2\pi \beta_0} \ln(1 - \lambda) - \frac{\gamma_{qq}(N)}{\pi \beta_0} \ln(1 - \lambda) + \frac{2C_F}{\pi \beta_0} \frac{\lambda}{1 - \lambda} (-\ln 2) \\ &\quad + \frac{K C_F [\lambda + (1 - \lambda) \ln(1 - \lambda)]}{2\pi^2 \beta_0^2 (1 - \lambda)} - \frac{C_F \beta_1}{\pi \beta_0^3} \left[\frac{\lambda + \ln(1 - \lambda)}{1 - \lambda} + \frac{1}{2} \ln^2(1 - \lambda) \right], \quad (2.79) \end{aligned}$$

with $\lambda = \alpha_s(M^2) \beta_0 L$.

Let us comment on the origin of various terms. The leading logarithmic function $g_1(\lambda)$ arises from soft and collinear emission integrated over the phase space with a running coupling (to be precise the one-loop running of the coupling is sufficient to give us g_1). It is identical to the corresponding function for Z boson p_T resummation and at this level the a_T and p_T variables do not differ. The function g_2 embodies hard-collinear radiation (and hence the appearance of the quark anomalous dimension $\gamma_{qq}(N)$) as well as the two-loop running of the coupling and the change to the $\overline{\text{MS}}$ scheme from the CMW scheme which gives rise to the piece proportional to K . It is also the same as the corresponding function for Z boson p_T resummation *except* for the additional single-logarithmic term $\frac{2C_F}{\pi \beta_0} \frac{\lambda}{1 - \lambda} (-\ln 2)$ which arises from the ϕ dependence of the problem. In other words one has ex-

plicitly

$$\frac{\partial R_{\text{LL}}(\bar{b})}{\partial \ln(\bar{b}M)} \int_0^{2\pi} \frac{d\phi}{2\pi} \ln |\sin \phi| = \frac{\partial L g_1(\lambda)}{\partial \ln(\bar{b}M)} (-\ln 2) = \frac{2C_F}{\pi\beta_0} \frac{\lambda}{1-\lambda} (-\ln 2). \quad (2.80)$$

However, this term, within NLL accuracy, can be absorbed in the radiator with a change in the definition of its argument \bar{b} :

$$R(\bar{b}) + \frac{\partial R_{\text{LL}}(\bar{b})}{\partial \ln(\bar{b}M)} \int_0^{2\pi} \frac{d\phi}{2\pi} \ln |\sin \phi| = R(\bar{b}) - \frac{\partial R_{\text{LL}}(\bar{b})}{\partial \ln(\bar{b}M)} \ln 2 \simeq R(\bar{b}/2), \quad (2.81)$$

and $R(\bar{b}/2) = R(b e^{\gamma_E}/2)$ is precisely the radiator for the Z boson p_T distribution (see e.g. Ref. [27]). As a final step we can use the anomalous dimension matrix $\gamma_{qq}(N)$ and the corresponding contribution $\gamma_{qg}(N)$ from Compton scattering which we have for brevity avoided treating, to evolve the pdfs from scale M^2 to scale $(2/\bar{b})^2$ precisely as in the case of the p_T variable. After absorption of the N dependent piece of the radiator into a change of scale of the pdfs it is trivial to invert the Mellin transform to go from N space to τ space. We can thus schematically write the result for the a_T cross-section defined in (2.5) resummed to NLL accuracy as

$$\begin{aligned} \Sigma(a_T, M^2) &= \mathcal{G} \frac{M^2}{3\pi} \frac{A_l A_q}{N_c} \frac{2}{\pi} \int_0^\infty \frac{db}{b} \sin(ba_T) \exp(-S(\bar{b}/2)) \times \\ &\times \int_0^1 dx_1 \int_0^1 dx_2 [f_q(x_1, (2/\bar{b})^2) f_{\bar{q}}(x_2, (2/\bar{b})^2) + q \leftrightarrow \bar{q}] \delta(M^2 - x_1 x_2 s). \end{aligned} \quad (2.82)$$

Problems related to the small and large b regions of this integral will be discussed later, in section 2.9. The function $S(\bar{b}/2)$ is just the radiator $R(\bar{b})$ without the N dependent anomalous dimension terms which have been absorbed into the pdfs:

$$S(\bar{b}/2) = 2C_F \int_{(2/\bar{b})^2}^{M^2} \frac{dk_t^2}{k_t^2} \frac{\alpha_s(k_t^2)}{2\pi} \left(\ln \frac{M^2}{k_t^2} - \frac{3}{2} \right). \quad (2.83)$$

As we just pointed out this function coincides with the corresponding function in the p_T case. All differences between a_T and p_T thus arise from the fact that one has

to convolute the resummed exponent and pdfs with a sine function representing the constraint on a single component of k_t , rather than a Bessel function representing a constraint on both components of the k_t . Having achieved the resummation we shall next expand our resummed result to order α_s^2 and compare its expansion to fixed-order results to non-trivially test the resummation.

2.8 Comparison to fixed-order results

In order to non-trivially test the resummation we have the option of expanding the results to order α_s^2 (i.e. up to two-loop corrections to the Born level) and testing the logarithmic structure against that emerging from fixed-order calculations. Since the results for the p_T distribution are already well-known and since many terms are common to the a_T and p_T resummed results it is most economical to provide a prediction for the difference between the a_T and p_T variables. To be precise we already identified a leading-order result for the difference between cross-sections involving a_T and $p_T/2$ in Eq. (2.57). In this section we shall derive this difference at NLO level and compare to fixed-order estimates.

Let us consider the resummed results for the a_T and $p_T/2$ cases. We remind the reader of the well-known result for the p_T variable by expressing the integrated cross-section for events with $p_T/2$ below a fixed value ϵM :

$$\Sigma(p_T/2) |_{p_T/2=\epsilon M} = \left(1 + C_1(N) \frac{\alpha_s}{2\pi}\right) \tilde{\Sigma}^{(0)}(N) \int_0^\infty db 2M\epsilon J_1(b 2M\epsilon) e^{-R(\frac{b}{2})}, \quad (2.84)$$

The above result is expressed in moment space and we have additionally provided a multiplicative coefficient function $(1 + C_1(N) \alpha_s/(2\pi))$, so that the result accounts also for constant terms at leading order. This form of the resummation

is correct up to NNLL accuracy in the cross-section whereas the pure resummed result without the multiplicative constant piece is correct to NLL accuracy in the resummed exponent [43]. Thus with the constant C_1 in place the resummation should guarantee at order α_s^2 terms varying as $\alpha_s^2 L^4$, $\alpha_s^2 L^3$ as well as the $\alpha_s^2 L^2$ term which partially originates from a “cross-talk” between the $\alpha_s C_1$ term and the $\alpha_s L^2$ term in the expansion of the exponent.¹⁰

The equivalent result for the a_T variable is

$$\Sigma(a_T)|_{a_T=\epsilon M} = \left(1 + \bar{C}_1(N) \frac{\alpha_s}{2\pi}\right) \tilde{\Sigma}^{(0)}(N) \frac{2}{\pi} \int_0^\infty \frac{db}{b} \sin(bM\epsilon) e^{-R(\frac{b}{2})}, \quad (2.85)$$

where \bar{C}_1 is the constant for the a_T variable. We shall first expand the resummation to order α_s and consider the difference between a_T and $p_T/2$. First we express the radiator in the standard notation [43]

$$-R(\bar{b}/2) = \sum_{n=0}^{\infty} \sum_{m=0}^{n+1} G_{nm} \bar{\alpha}_s^n L^m, \quad L = \ln(\bar{b}^2 M^2/4), \quad (2.86)$$

with $\bar{\alpha}_s = \alpha_s/2\pi$. Having done so we expand the resummed exponent so that to order α_s we can write for the p_T variable

$$\begin{aligned} \Sigma(p_T/2)|_{p_T/2=\epsilon M} &= (1 + C_1(N) \bar{\alpha}_s) \tilde{\Sigma}^{(0)}(N) \int_0^\infty db 2M\epsilon J_1(b 2M\epsilon) \times \\ &\times \left(1 + G_{11} \bar{\alpha}_s L + G_{12} \bar{\alpha}_s L^2 + \mathcal{O}(\alpha_s^2)\right), \end{aligned} \quad (2.87)$$

where we replaced the resummed exponent by its expansion to order α_s .

¹⁰This form of the result we use is an oversimplification since we consider only the piece of the $\mathcal{O}(\alpha_s)$ constant which is associated to the annihilation channel. In principle one should also include the constant arising from the Compton channel but this is identical to the corresponding constant for the p_T variable [35] and it is straightforward to show that its effects cancel to the accuracy we need for the result we derive below for the difference between a_T and $p_T/2$ variables.

Carrying out the b integral yields

$$\Sigma(p_T/2)|_{p_T/2=\epsilon M} = (1 + C_1(N)\bar{\alpha}_s) \tilde{\Sigma}^{(0)}(N) \left(1 + G_{11}\bar{\alpha}_s \ln \left[\frac{1}{4\epsilon^2} \right] + G_{12}\bar{\alpha}_s \ln^2 \left[\frac{1}{4\epsilon^2} \right] \right), \quad (2.88)$$

where for the moment we do not insert the explicit forms of the G_{nm} coefficients.

Repeating the exercise for the a_T variable one obtains

$$\begin{aligned} \Sigma(a_T)|_{a_T=\epsilon M} &= (1 + \bar{C}_1(N)\bar{\alpha}_s) \tilde{\Sigma}^{(0)}(N) \times \\ &\times \left(1 + G_{11}\bar{\alpha}_s \ln \left[\frac{1}{4\epsilon^2} \right] + G_{12}\bar{\alpha}_s \ln^2 \left[\frac{1}{4\epsilon^2} \right] + G_{12}\bar{\alpha}_s \frac{\pi^2}{3} \right), \end{aligned} \quad (2.89)$$

where we labeled the constant piece as \bar{C}_1 to distinguish it from that for the p_T variable. Constructing the difference at $\mathcal{O}(\alpha_s)$ between the a_T and $p_T/2$ variables we find that all the logarithms cancel and we obtain

$$\Sigma(a_T)|_{a_T=\epsilon M} - \Sigma(p_T/2)|_{p_T/2=\epsilon M} = \tilde{\Sigma}^{(0)}(N) \bar{\alpha}_s \left(\bar{C}_1(N) - C_1(N) + G_{12} \frac{\pi^2}{3} \right). \quad (2.90)$$

The value of the resummation coefficient G_{12} can be obtained from Eq. (2.79) by expanding the result in powers of λ from which we find $G_{12} = -C_F$. Comparing this result with our explicit leading order calculation Eq. (2.57) we find that $C_1 = \bar{C}_1$.

Next we carry out the expansion of our resummation to order α_s^2 and construct the difference from $p_T/2$ at this order. We shall then compare our expectation with MCFM. Expanding the radiator to order α_s^2 one gets

$$\begin{aligned} e^{-R(\frac{\bar{b}}{2})} &= 1 + \bar{\alpha}_s (G_{11}L + G_{12}L^2) \\ &+ \bar{\alpha}_s^2 \left(\frac{G_{11}^2 L^2}{2} + G_{22}L^2 + G_{11}G_{12}L^3 + G_{23}L^3 + \frac{G_{12}^2 L^4}{2} \right). \end{aligned} \quad (2.91)$$

Retaining only the $\mathcal{O}(\alpha_s^2)$ terms we can once again carry out the b space integrals as before and in particular the new integrals that appear at this order

are

$$\begin{aligned}
I_{a_T}^{(p)} &= \frac{2}{\pi} \int_0^\infty \frac{db}{b} \sin(bM\epsilon) \ln^p \left(\bar{b}^2 \frac{M^2}{4} \right), \\
I_{p_T}^{(p)} &= \int_0^\infty db 2M\epsilon J_1(b 2M\epsilon) \ln^p \left(\bar{b}^2 \frac{M^2}{4} \right),
\end{aligned} \tag{2.92}$$

with $p = 3, 4$. Carrying out the above integrals with $p = 3$ is straightforward and the difference between the integrals for the p_T and a_T case with $p = 3$ produces only an $\alpha_s^2 \ln 1/\epsilon^2$ term apart from constant pieces. Such terms are beyond the accuracy of our resummation which ought to guarantee only terms as singular as $\alpha_s^2 \ln^2 1/\epsilon^2$ in the cross-section and hence to our accuracy there will be no contribution for $p = 3$ for the difference between a_T and $p_T/2$.

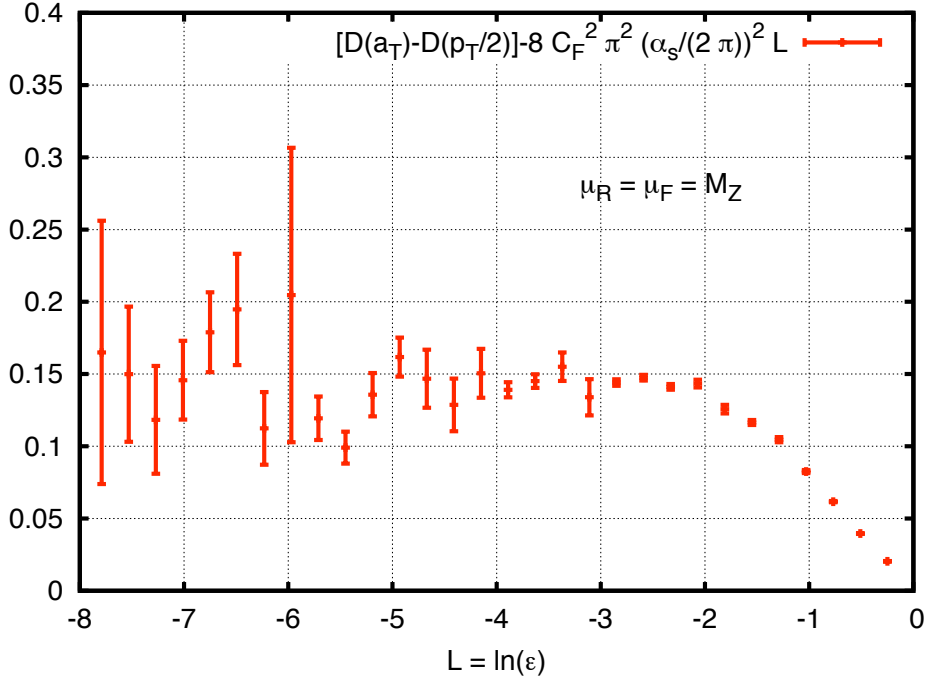


Figure 2.5: The difference between $D(a_T)$ and $D(p_T/2)$, defined in Eq. (2.94) with the subtraction of the computed logarithmic enhanced term in Eq. (2.93).

The situation changes when we consider the $p = 4$ integrals. All relevant loga-

arithms cancel between a_T and $p_T/2$ once again except a term varying as $\alpha_s^2 \ln^2 \frac{1}{\epsilon^2}$.

To be precise considering only the order α_s^2 terms one obtains

$$\begin{aligned} \Sigma(a_T)|_{a_T=\epsilon M} - \Sigma(p_T/2)|_{p_T/2=\epsilon M} &= \frac{G_{12}^2}{2} \times 2\pi^2 \bar{\alpha}_s^2 \ln^2 \frac{1}{\epsilon^2} \times \tilde{\Sigma}^{(0)}(N) + \mathcal{O}(\alpha_s^2 L) \\ &= \pi^2 \bar{\alpha}_s^2 C_F^2 \ln^2 \left(\frac{1}{\epsilon^2} \right) \times \tilde{\Sigma}^{(0)}(N). \end{aligned} \tag{2.93}$$

To convert the result above back into τ space from Mellin space is straightforward as one just inverts the Mellin transform for $\tilde{\Sigma}^{(0)}$ to yield the Born-level quantity $\Sigma^{(0)}$ as the multiplicative factor.

Once again the above result can be tested against the results from MCFM. We consider the difference in the differential distributions (derivative with respect to $\ln \epsilon$ of the appropriate integrated cross-sections) for a_T and $p_T/2$ as a function of $\ln \epsilon$

$$D(a_T)|_{a_T=\epsilon M} - D(p_T/2)|_{p_T/2=\epsilon M} = \frac{1}{\Sigma^{(0)}} \left[\frac{d\Sigma(a_T)}{d \ln \epsilon} \Big|_{a_T=\epsilon M} - \frac{d\Sigma(p_T/2)}{d \ln \epsilon} \Big|_{p_T/2=\epsilon M} \right]. \tag{2.94}$$

Our prediction for this difference can be obtained by taking the derivative with respect to $\ln \epsilon$ of the RHS of Eq. (2.93). Subtracting this prediction from the MCFM results should yield at most constant terms arising from the logarithmic derivative of formally subleading $\alpha_s^2 \ln \epsilon$ terms. That this is the case can be seen from Fig. 2.5 where we note that at sufficiently small values of ϵ the difference between MCFM and our prediction tends to a constant.

2.9 Discussion and conclusions

Before concluding we should comment on the resummed result Eq. (2.82). First we note that there is the usual issue that is involved with b space resummation of

the large and small b behaviour of the integrand in that the resummed exponent diverges in both limits. The small b region is conjugate to the large k_t regime which is beyond the jurisdiction of our resummation. At sufficiently large b on the other hand we run into non-perturbative effects to do with the Landau pole in the running coupling. These issues can be resolved by modifying the radiator such that the perturbative resummation is not impacted. For instance the strategy adopted in Ref. [32] was to replace the resummation variable b by another variable b^* which coincides with b in the large b limit but at small b ensures that the radiator goes smoothly to zero. Likewise to regulate the Landau pole a cut-off was placed in the large b region of integration in the vicinity of the Landau pole and it was checked that varying the position of the cut-off had no impact on the resummation. Other prescriptions can be found for instance in [44].

As far as the behaviour of the resummed cross-section and consequently the corresponding differential distribution is concerned the difference from the p_T distribution is solely due to the convolution of the resummed b space function with the $\sin(b)$ function rather than a Bessel function. As was explained in detail in Ref. [41] the result of convolution with a sine function produces a distribution that does not have a Sudakov peak. The physical reason for this is that a small value of a_T can be obtained by two competing mechanisms. One mechanism is Sudakov suppression of gluon radiation and this is encapsulated to NLL accuracy by the resummed exponent. The other mechanism is the vectorial cancellation of contributions from arbitrarily hard emissions which in this case involves cancellation only of a single component of k_t transverse to the lepton axis. This mechanism is represented by the presence of the sine function while a two-dimensional constraint such as that for the p_T variable is represented by a Bessel function. In the case of

one dimensional cancellation such as for the a_T as well as for instance for the dijet $\Delta\phi$ variable [30] the cancellation mechanism dominates the Sudakov suppression mechanism before the formation of the Sudakov peak while for the p_T case the vectorial cancellation sets in as the dominant mechanism after the formation of the Sudakov peak. Thus for the a_T distribution one sees no Sudakov peak but the distribution rises monotonically to a constant value as predicted by Eq. (2.82).

To conclude, in this chapter we have carried out a theoretical study based on a variable, a_T proposed in Ref. [9] as an accurate probe of the low p_T region of the Z boson. Having accurate data on the a_T well into the low a_T domain will be invaluable in pinning down models of the non-perturbative intrinsic k_t and may lead to firmer conclusions on aspects such as small- x broadening of p_T distributions [15] than have been reached at present with the p_T variable. In this respect it may also be of interest to examine theoretically the power corrections to the a_T distribution along the same lines as for the p_T case [45] and hence to examine theoretically whether the a_T and p_T ought to have identical non-perturbative behaviour. This is once again work in progress.

Before any such conclusions can be arrived at however, it is of vital importance to have as accurate a perturbative prediction as possible to avoid misattributing missing perturbative effects to other sources. The most accurate perturbative prediction one can envisage for the a_T case is where resummation of large logarithms in a_T is supplemented by matching to fixed-order corrections up to the two-loop level. In this thesis we have carried out the first step by resumming to NLL accuracy and checking our resummation by comparing to the logarithmic structure in exact fixed order calculations. In a recent paper the accuracy of the resummation was extended to the NNLL level [46]. Besides, another variable, the

angle-between-leptons distribution in Drell-Yan processes ϕ^* [47] has also been recently computed [48] as a more accurate probe of the low p_T domain of Z boson production at hadron colliders. A next-to-next-to leading logarithmic (NNLL) resummation was matched to a fixed order calculation at next-to-leading order (NLO). This theoretical prediction was found to be in good agreement with the measurement by the DØ collaboration [49]. These and future studies will shed more light on issues relevant to physics at the LHC in the near future.

Chapter 3

Gaps between jets at the LHC

QCD phenomenology and in particular jet physics are playing a central role in the physics program of the first period of the LHC running [50–56]. While the predictions of inclusive jet and dijet cross sections are under good perturbative control, the prediction of the associated final states is much more delicate. A crucial role is played by the colour structure of the hard process, which sets the initial conditions both of the parton shower, which describes the perturbative evolution of the event, and the hadronization, which describes the transition of those partons into the hadrons that are seen in the final state (for an overview of this physics, see for example [57]). While long viewed as a probe of QCD dynamics (as outlined in Fig. 3.1), it has only more recently become widely realized that a measurement of hard process colour structure could be an important probe of new physics [58–61] (although the idea dates back to at least [62]).

The most direct probe of the colour structure of a hard process is the probability that it does not radiate into some well-defined region of phase space. In this chapter we consider the prototypical process, in which a dijet system is measured and the presence of any additional jets in the inter-jet region is vetoed. The inter-

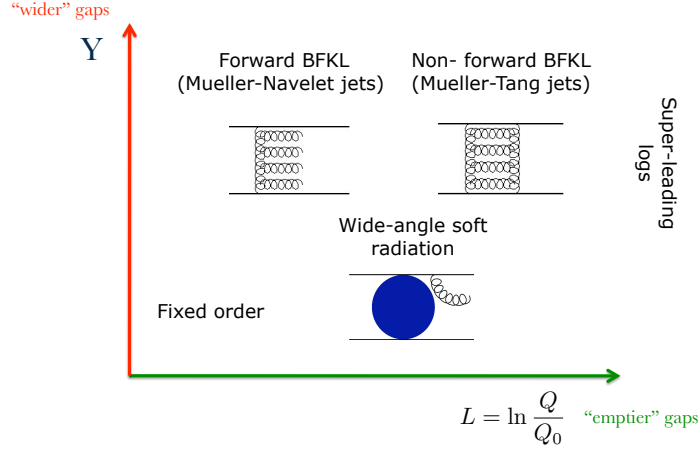


Figure 3.1: Range of QCD phenomena as a function of $L = \ln(Q/Q_0)$ and Y , where Q is the transverse momentum of the leading jets, Q_0 the veto scale and Y the gap rapidity separation. Figure from Ref. [63].

jet region is referred as the rapidity interval between the two jets produced with highest transverse momentum, named *leading* jets. More precisely, we define gap events as those that present no additional inter-jet radiation with transverse energy greater than a given *veto scale*, as illustrated in Fig. 3.2.

The fraction of dijet events with an observed rapidity gap (the jet veto “gap fraction”) has been measured by the Tevatron and HERA collaborations [64–68] and, very recently, for the first time at the LHC [52]. Historically, “gaps between jets” (as it has come to be called) was studied to find evidence for the existence of a strongly interacting colour-singlet object, the *perturbative Pomeron*. At the LHC, gaps between jets will likely play an important role in studies of the colour-singlet *Higgs* boson. The two expected dominant channels for Higgs production at the

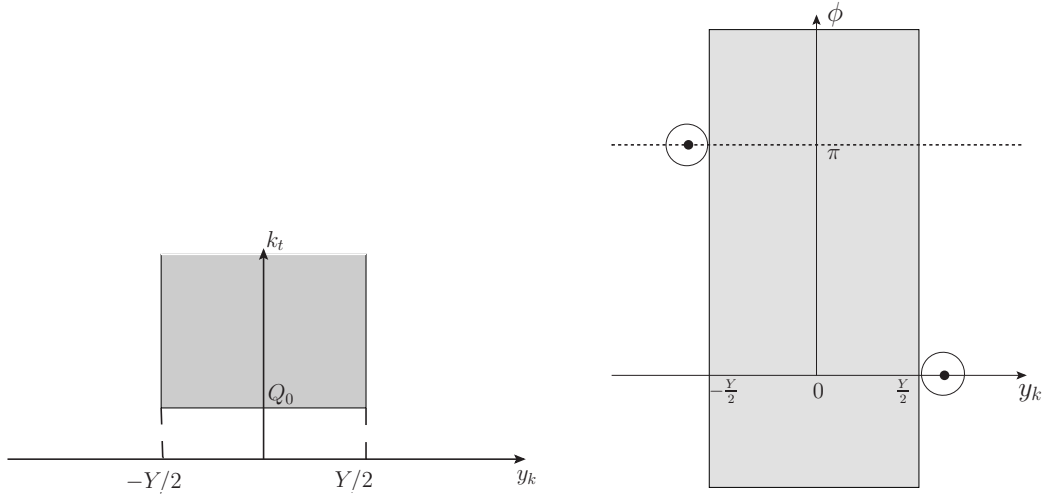


Figure 3.2: Representations of the (shaded) veto region for the emission of gluons of rapidity $|y_k| < Y/2$, transverse momentum $k_t > Q_0$ and azimuth ϕ_k , where Y is the gap size and Q_0 the veto scale. In the second diagram the two outgoing jets are represented with two circles of radius $R = \Delta y/2 - Y/2$, where Δy is the dijet rapidity separation.



Figure 3.3: The dominant mechanisms for Higgs production at the LHC: (left) gluon fusion, via a top quark loop; (right) vector-boson fusion.

LHC are gluon fusion (GF) and vector-boson fusion (VBF), sketched in Fig. 3.3. Although VBF is not the strongest channel, its signal is the cleanest, since VBF is a colour-singlet exchange process, while GF, the dominant channel, is a pure QCD interaction and radiation between the jets is much more likely to occur. Thus, in Higgs production in association with two jets, VBF can be relatively

enhanced by imposing a veto on the radiation between the two jets [61, 69, 70]. Besides, if one aims to extract values for the Higgs couplings it is important to get reliable theoretical calculations of the fraction of VBF and GF events [71]. A good understanding of gaps between jets in dijet events will help to constrain this modeling, given that the colour structure for the production of Higgs boson in association with two jets is almost identical to the dijet processes that we study here [72].

The cross section for gaps events can be calculated perturbatively, provided the threshold for reconstructing and vetoing jets is in the perturbative regime. However, at every order of perturbation theory, logarithms of the ratio of the hard process scale to this jet veto threshold scale arise, and when this ratio is large it is mandatory to sum these logarithms to all orders. When the ratio of scales is not large, these logarithms do not dominate and fixed order perturbative results are more accurate than the resummed results (bottom left corner of Fig. 3.1). To provide a prediction that is valid over all values of the ratio, it is necessary to match the resummed and fixed-order calculations, which is one of our aims here.

In Ref. [73] a first phenomenological study of this observable was made, comparing the resummation of soft gluons to a standard event generator (HERWIG++ [16]). It was found that neither approach was completely satisfactory. The parton shower simulation does not contain the full colour structure or any account of the mixing between different colour structures, and neglects contributions coming from loop corrections that do not correspond to a non-emission contribution (so-called Coulomb gluon exchanges). These give a sizable correction at large enough jet transverse momenta and rapidity separation. Moreover, higher than expected non-emission probabilities were found, which has more recently [74] been

explained as a problem with the way HERWIG++ implements the colour structure of hard processes involving gluons. On the other hand, the resummation approach, which is based on the soft gluon approximation, by itself is not sufficient for currently-probed phase-space regions. One important effect that it neglects is energy-momentum conservation: within the soft gluon approximation, the additional jets that one is vetoing could be emitted with a suppression only due to matrix elements, whereas in full QCD such emission would be suppressed by the requirement that it carry away enough energy that it be above the jet veto scale.

In the calculations presented in this chapter (published in [75]), we improve the previous resummed predictions for the gap fraction by modifying them to approximately account for energy-conservation effects and by matching them to the leading QCD order calculation. We also include the first tower of non-global logarithms arising from one gluon emission outside of the gap region.

In the next section, we make a quick revision of the main formulae used to calculate general dijet cross-sections. Then we continue reviewing some general ideas on soft-gluon emission and how to account for it. Following that, we define more precisely the observable that we will calculate: the gap fraction. We then discuss the all-orders resummation of the associated leading logarithms, and how to match this result with a fixed-order result. Finally, we compare the matched results with the ATLAS data and with other theoretical predictions, before drawing some conclusions.

3.1 Cross-section for dijet production

Our aim is to calculate the inclusive cross-section of dijet production in proton-proton collisions, $h_1 + h_2 \rightarrow jj + X$, with a veto on the emission of extra jets;

specifically we are vetoing radiation with rapidities $|y_k| < Y/2$ and transverse momenta $k_t > Q_0$, where Y and Q_0 are the rapidity size of the gap and the veto scale respectively.

Concerning the kinematics of the events, we consider the two leading jets to be produced back to back as a first approximation. This assumption relies on the fact that radiative corrections in the dijet system will only have a significant effect in the cross-section if it is soft, i.e., if its energy is negligible in comparison with the hard scale of the process; in that case the process may be described as having the Born kinematics, $h_1 + h_2 \rightarrow jj$ ¹. The formula to obtain the gaps between jets (GBJ) cross-section will then be identical to that for dijet production. The effect of vetoing radiation in the inter-jet region will only appear as logarithmic corrections in the squared matrix elements, as we will see.

The cross-section for dijet production is given by

$$\sigma = \frac{1}{2S} \int g^4 \frac{f_a(x_1, Q^2)}{x_1} \frac{f_b(x_2, Q^2)}{x_2} dx_1 dx_2 \sum_{a,b,c,d} \frac{1}{1 + \delta_{ab}} \frac{1}{1 + \delta_{cd}} |\mathcal{M}_{abcd}|^2 d\Phi, \quad (3.1)$$

where the indices a, b and c, d refer to the flavours of the initial- and final-state partons respectively and $d\Phi$ is the two-body phase-space. The coupling factors g^4 have been factored out of the matrix element for future convenience. The pdfs are evaluated at scale Q , which we set to be the mean transverse momentum of the leading jets, and at the following longitudinal-momentum fractions:

$$x_1 = \sqrt{z} \exp(\bar{y}/2), \quad x_2 = \sqrt{z} \exp(-\bar{y}/2), \quad (3.2)$$

¹In the soft approximation, energy-momentum is conserved only in the limit of soft gluon emission. The reliability of this assumption should ideally be studied in more depth, since the radiation included in the resummation presented here must have transverse momentum $k_t > Q_0$. The value of Q_0 is commonly chosen to be $Q_0 = 20$ GeV in order to reduce contamination from the underlying event; Q_0 could in principle be lowered once those effects are better understood.

where \bar{y} is the sum of the rapidities of the two outgoing jets and we define

$$z = x_1 x_2 = 4Q^2/S \cosh^2 \Delta y/2. \quad (3.3)$$

Hence, the cross-section distribution can be calculated from the following formula:

$$\frac{d^3\sigma}{dQ^2 d\Delta y} = \frac{\pi \alpha_s^2(Q)}{S^2} \frac{1}{1 + \delta_{ab}} \frac{1}{1 + \delta_{cd}} |\mathcal{M}_{abcd}|^2 \int_{-\bar{y}^+}^{\bar{y}^+} \frac{d\bar{y}}{2} \frac{f_a(x_1, Q^2) f_b(x_2, Q^2)}{z}. \quad (3.4)$$

The \bar{y} integration limits are derived from the usual kinematic constraints $x_1, x_2 < 1$, together with the maximum rapidity value detectable at the experiment; the upper-integration limit is thus given by

$$\bar{y}^+ = \min\left(\ln \frac{1}{z}, \bar{y}_{\text{cut}}\right) \quad (3.5)$$

and the value $\bar{y}_{\text{cut}} = 2\eta - \Delta y$ is obtained by requiring that both jets are within the LHC hadronic calorimeter acceptance, i.e. $\eta = 4.9$.

3.2 Colour-basis independent notation

Hadronic processes that end up with two or more partons in the final state often involve a rather complex colour structure; it can then be convenient to work using a tensorial notation (see [76–80] for examples), without specifying a particular colour basis. Only at a final stage in the calculation we will need to choose a basis in order to get actual numbers and compare them with experimental results; the challenge at that stage is to find a suitable basis.

As we mentioned in the introduction, the theory of QCD is constructed based on the idea that colour charge is conserved in hadronic interactions. In tensorial notation this can be expressed as follows:

$$|m\rangle = e^{i\mathbf{a}\cdot\mathbf{T}} |m\rangle,$$

where $|m\rangle$ represents a matrix element of m partons, and $e^{i\mathbf{a}\cdot\mathbf{T}}$ is a general transformation (or rotation) given by the $SU(N_c)$ tensors \mathbf{T} through the “angles” \mathbf{a} . In other words, this formula tells us that

$$(\mathbf{1} - e^{i\mathbf{a}\cdot\mathbf{T}}) |m\rangle = \mathbf{0},$$

which implies

$$\mathbf{a} \cdot \mathbf{T} |m\rangle = \mathbf{0},$$

to a first approximation.

Now, since colour conservation of the hadronic system does not depend on the particular rotation performed on it, it follows that

$$\mathbf{T} |m\rangle = \mathbf{0}. \tag{3.6}$$

This result expresses colour conservation and will be useful later.

Let us now see how a general hadronic process is affected by initial or final-state radiation of gluons and how we can represent this effect in a colour basis independent notation. In particular, in our calculation, we will be interested in computing the impact of adding *virtual* gluon exchanges (integrated over the veto region) to the original process of dijet production.

3.2.1 Soft gluon emission

Let us now consider that we address the amplitude $|m\rangle$ for a gap event of m final-state partons with the radiation of a virtual soft gluon. The partons involved in the interaction are sketched in Fig.3.4.

For simplicity, let us first consider the emission of a soft real gluon; the amplitude transforms as

$$|m+1\rangle = g \sum_i \frac{p_i \cdot \epsilon^*}{p_i \cdot k} \mathbf{T}_i^a |m\rangle, \tag{3.7}$$

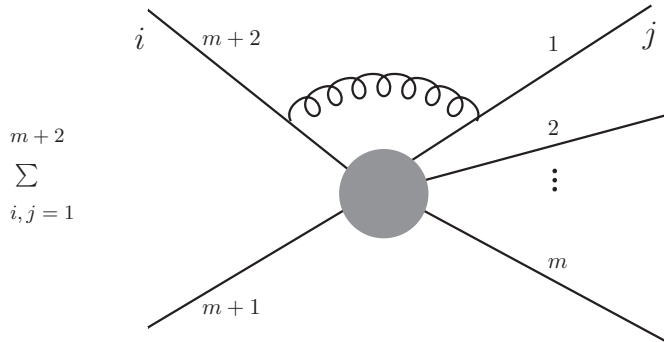


Figure 3.4: Exchange of a virtual gluon between any two incoming or outgoing partons.

where k is the momentum of the emitted gluon and ϵ is its polarization vector. The tensors \mathbf{T}_i^a , map the m dimensional vector space onto the $m + 1$ dimensional space (original process plus an extra gluon). They are given by

$$\mathbf{T}_i^a = \begin{cases} \mathbf{t}^a & \text{if parton } i \text{ is an outgoing quark or an incoming antiquark} \\ -\mathbf{t}^a & \text{if parton } i \text{ is an incoming quark or an outgoing antiquark} \\ -i\mathbf{f}^a & \text{if parton } i \text{ is a gluon} \end{cases} ,$$

where \mathbf{t}^a are the $SU(N_c)$ generators in the fundamental representation and $-i\mathbf{f}^a$ are the generators in the adjoint representation.

Now, let us see how the original amplitude transforms with the emission of a soft *virtual* emission. The Bloch-Nordsieck theorem [81] states that the singularities coming from virtual and real gluon emission cancel against each other. This has the corollary that the accompanying logarithms cancel for sufficiently inclusive observables. In gaps between jets events, however, we veto the real gluon emission in the gap region. We can account for this miscancellation by resumming the logarithmic corrections coming from virtual gluon emission in the inter-jet region. We thus need to integrate the momentum of the virtual gluon over the “non-

cancelling” region of phase space, i.e. over the veto region. This leads us to the following formula:

$$\mathbf{\Gamma} = - \sum_{i < j} \mathbf{T}_i \cdot \mathbf{T}_j \Omega_{ij}. \quad (3.8)$$

For an azimuthal-symmetric gap, Ω_{ij} is given by

$$\Omega_{ij} = \frac{1}{2} \left\{ \int_{\text{veto}} \frac{dy d\phi}{2\pi} \omega_{ij} - i\pi \Theta(ij = II \text{ or } FF) \right\}, \quad (3.9)$$

the sum over i, j runs over all partons in the initial and final state, and the theta function ensures that the $i\pi$ contribution is present only when ij correspond to a pair of incoming (II) or outgoing (FF) partons. The kinematic function ω_{ij} is defined as follows:

$$\omega_{ij} = \frac{1}{2} k_T^2 \frac{p_i \cdot p_j}{(p_i \cdot k)(p_j \cdot k)}. \quad (3.10)$$

The so-called soft anomalous dimension $\mathbf{\Gamma}$ is a matrix, with elements $\Gamma_{ij} = \langle e_i | \mathbf{\Gamma} | e_j \rangle$ in a basis $\{e_i\}$:

$$\begin{aligned} \mathbf{\Gamma} &= -\frac{1}{2} \int_{\text{veto}} \frac{d\phi}{2\pi} dy \left[\mathbf{t}_a \cdot \mathbf{t}_b \omega_{12} + \mathbf{t}_a \cdot \mathbf{t}_c \omega_{13} + \mathbf{t}_a \cdot \mathbf{t}_d \omega_{14} \right. \\ &\quad \left. + \mathbf{t}_b \cdot \mathbf{t}_c \omega_{23} + \mathbf{t}_b \cdot \mathbf{t}_d \omega_{24} + \mathbf{t}_c \cdot \mathbf{t}_d \omega_{34} \right] + i\pi \mathbf{t}_a \cdot \mathbf{t}_b, \\ \omega_{ij} &= \frac{1}{2} k_T^2 \frac{p_i \cdot p_j}{p_i \cdot k p_j \cdot k}, \end{aligned} \quad (3.11)$$

where \mathbf{t}_i is the colour charge of parton i^2 . The soft gluon momentum is labeled k . The integrals over the gluon’s azimuth and rapidity inside the gap region admit simple analytical expressions if one considers azimuthal symmetric gaps. However, in the current analysis, we are defining the gap from the centres of the leading jets. Thus, the gap region is not just a rectangle in the (η, ϕ) plane and we have to

²Note that the mismatch between the indices $1, 2, \dots$ and a, b, \dots is related to the fact that one must sum over two orientations of the event, e.g. $i(p_1, \mathbf{t}_a) + j(p_2, \mathbf{t}_b) \rightarrow k(p_3, \mathbf{t}_c) + l(p_4, \mathbf{t}_d)$ and $i(p_1, \mathbf{t}_a) + j(p_2, \mathbf{t}_b) \rightarrow l(p_3, \mathbf{t}_d) + k(p_4, \mathbf{t}_c)$, as explained in more detail in [73].

integrate around the two semi-circular boundaries of the leading jets. Analytical expressions can still be obtained as a power series in R [82]. Here instead we decide to keep the full R dependence and perform the integrals numerically when we cannot find simple analytical results. For the explicit expressions of the hard scattering matrices H in the various partonic channels we refer to [73].

By integrating explicitly over (ϕ, y) and after exploiting colour conservation Eq. (3.6), the soft anomalous dimension for four-parton evolution reduces to

$$\mathbf{\Gamma} = \frac{1}{2}Y\mathbf{t}_t^2 + i\pi\mathbf{t}_a \cdot \mathbf{t}_b + \frac{1}{4}\rho(Y; |\Delta y|)(\mathbf{t}_c^2 + \mathbf{t}_d^2), \quad (3.12)$$

where

$$\rho(Y; \Delta y) = \ln \frac{\sinh(\Delta y/2 + Y/2)}{\sinh(\Delta y/2 - Y/2)} - Y, \quad (3.13)$$

and $\mathbf{t}_t = \mathbf{t}_a + \mathbf{t}_c$ is the colour charge matrix corresponding to emission from the total colour exchanged in the t channel.

3.2.2 Mapping onto a particular colour basis

Let us consider a particular colour basis suitable for describing quark-quark scattering:

$$\begin{aligned}
e_1 &= \frac{1}{3}\delta_{ik}\delta_{jl} & e_2 &= \frac{1}{2\sqrt{2}}(\delta_{il}\delta_{jk} - \frac{1}{3}\delta_{ik}\delta_{jl}) \\
&= \frac{1}{3} \begin{array}{c} \overline{i} \quad \quad \quad \overline{k} \\ \hline \overline{j} \quad \quad \quad \overline{l} \end{array} & & = \frac{1}{2\sqrt{2}} \begin{array}{c} i \quad \quad \quad k \\ \curvearrowright \quad \quad \quad \curvearrowleft \\ j \quad \quad \quad l \end{array} & & - \frac{1}{6\sqrt{2}} \begin{array}{c} \overline{i} \quad \quad \quad \overline{k} \\ \hline \overline{j} \quad \quad \quad \overline{l} \end{array}
\end{aligned}$$

This basis is orthonormal, i.e.

$$\langle e_1|e_1 \rangle = 1, \quad \langle e_2|e_2 \rangle = 1 \quad \text{and} \quad \langle e_1|e_2 \rangle = 0.$$

We can compute the elements of the anomalous dimension matrix by projecting Eq. (3.12) onto this basis. For example, for the scattering of non-identical quarks, $qq' \rightarrow qq'$, we obtain the following:

$$\mathbf{\Gamma} = \begin{pmatrix} \frac{2}{3}\rho_{\text{jet}} & \frac{i\pi\sqrt{2}}{3} \\ \frac{i\pi\sqrt{2}}{3} & \frac{2}{3}\rho_{\text{jet}} + \frac{3}{2}Y - \frac{i\pi}{3} \end{pmatrix}. \quad (3.14)$$

We can also project the hard scattering matrix onto this basis at the Born level corresponding to this sub-process,

$$H(t, u) = \frac{4}{9} \begin{pmatrix} 0 & 0 \\ 0 & \frac{u^2+s^2}{t^2} \end{pmatrix}. \quad (3.15)$$

An exhaustive list with all soft anomalous dimension and hard matrix elements for each partonic process can be found in Ref. [73].

3.3 The gap fraction

We are interested in dijet production in proton-proton collisions:

$$h_1(P_1) + h_2(P_2) \rightarrow j(p_3) + j(p_4) + X,$$

where we veto on the emission of a third jet with transverse momentum bigger than Q_0 in the rapidity region between the two jets. In the present study we fix the veto scale at $Q_0 = 20$ GeV. $P_{1,2}$ define the incoming hadron momenta and $p_{3,4}$ the outgoing jet momenta. We define the gap fraction as the ratio of the cross section for this process over the inclusive rate:

$$f^{\text{gap}} = \frac{d^2\sigma^{\text{gap}}}{dQ dY} / \frac{d^2\sigma}{dQ dY}. \quad (3.16)$$

In the Born approximation, the final state consists only of the two hard jets, so every event is a gap event and $f^{\text{gap}} = 1$. Beyond the Born approximation the

leading jets are no longer balanced in transverse momentum. We define Q to be the mean of the transverse momenta of the leading jets $Q = (p_{T3} + p_{T4})/2$. This choice, in contrast for instance to the transverse momentum of the leading jet, is more stable under the inclusion of radiative corrections [63]. The rapidity separation is defined by $Y = \Delta y - 2D$, where $\Delta y = |y_3 - y_4|$ is the rapidity separation between the centres of the leading jets and D can be freely chosen. In many previous studies, D was set equal to R , the jet radius. The ATLAS collaboration instead measure the gap region from the centres of the jets, i.e. $D = 0$ and thus $Y = \Delta y$. It is useful to rewrite Eq. (3.16) using unitarity:

$$\frac{d^2\sigma^{\text{gap}}}{dQ dY} + \frac{d^2\sigma^{\overline{\text{gap}}}}{dQ dY} = \frac{d^2\sigma}{dQ dY}, \quad (3.17)$$

where we have introduced the complement of the gap cross section, which corresponds to requiring at least one jet harder than Q_0 in the rapidity region in between the leading ones. The gap fraction then becomes

$$f^{\text{gap}} = 1 - \frac{d^2\sigma^{\overline{\text{gap}}}}{dQ dY} / \frac{d^2\sigma}{dQ dY}. \quad (3.18)$$

Our target in this chapter is to evaluate this expression at the first order in the strong coupling (LO) and to match it to the resummed calculation. At this accuracy then Eq. (3.18) contains only tree level contributions; the numerator is the integrated transverse momentum distribution of the third jet over the gap region and the denominator is simply the Born cross section:

$$f_{LO}^{\text{gap}} = 1 - \int_{Q_0}^Q dk_T \int_{\text{in}} dy d\phi \frac{d^5\sigma^{\overline{\text{gap}}}}{dk_T dy d\phi dQ dY} / \frac{d^2\sigma^{\text{born}}}{dQ dY} + \mathcal{O}(\alpha_s^2), \quad (3.19)$$

where k_T , y and ϕ are the transverse momentum, the rapidity and the azimuth of the third jet. The notation \int_{in} implies the integral over the gap region in rapidity and azimuth. We compute the gap fraction for proton-proton collisions at 7 TeV

using NLOJET++ [83] at leading order. The jets are defined using the anti- k_t algorithm [84] with $R = 0.6$. We use the CTEQ6.6 parton distribution functions (PDFs) [85] and adopt the same kinematical cuts as the ATLAS collaboration, requiring all jets to have $p_T > 20$ GeV and $|y| < 4.4$.

A fixed-order calculation of the gap fraction is reliable only at small Δy and when Q is of the same order as Q_0 . As soon as we move away from this region, the leading-order gap fraction decreases rapidly and eventually becomes negative. This unphysical behaviour indicates that the fixed order calculation by itself is not reliable. Large logarithms of the ratio Q/Q_0 contaminate the perturbative expansion and they must be resummed to all orders, as discussed in the next section. Also terms proportional to Δy (formally equivalent to a logarithm) can be resummed, for instance as in the High Energy Jets (HEJ) framework [86]. In the limit of large Δy and Q/Q_0 , the cross section is dominated by the singlet exchange component and there is overlap between the logarithms resummed by the approach we describe here and those resummed by the BFKL equation [87].

3.4 The resummed calculation

The technique for resumming logarithms of the ratio Q/Q_0 for the gaps-between-jets cross section has been explained in detail in [73,88–92]. It relies on the ability to map the real part of loop corrections into a form that is exactly equal and opposite to the phase space integral for real emission. For an observable in which emission is suppressed equally in all angular regions of the event, a global observable, there is an exact cancellation between the real and virtual contributions, such that the result (up to a phase term) is a virtual integral over the part of phase space in which real emission is vetoed.

In the observable we are studying, however, radiation is only suppressed in part of the phase space region and not globally. For this reason “in-gap” virtual corrections are not enough to capture even the leading logarithmic accuracy. Radiation outside the gap is prevented from re-emitting back into the gap by the veto requirement, inducing a further real–virtual miscancellation and additional towers of leading logarithms, called non-global logarithms [93]. Currently, these contributions can be resummed only in the large N_c approximation [94,95]. Here, instead we adopt the approach suggested by [91]: we keep the full colour structure but we expand in the number of gluons, real or virtual, outside the gap. It was argued in [73] that this may be a reasonably convergent expansion, so that the full result is approximated by the contributions arising from only zero or one gluons outside the gap:

$$\frac{d^2\sigma_{\text{res}}^{\text{gap}}}{dQ dY} = \frac{d^2\sigma^{(0)}}{dQ dY} + \frac{d^2\sigma^{(1)}}{dQ dY} + \dots \quad (3.20)$$

The first contribution to this expansion corresponds to the exponentiation of the one-loop virtual corrections (with no gluon outside the gap).

We define the resummed gap fraction as

$$f_{\text{res}}^{\text{gap}} = \frac{d^2\sigma_{\text{res}}^{\text{gap}}}{dQ dY} / \frac{d^2\sigma^{\text{born}}}{dQ dY}. \quad (3.21)$$

Because we are working in the eikonal approximation, additional radiation does not change the Born kinematics and the resummed cross section factorizes into products of resummed partonic contributions and parton luminosity functions:

$$\frac{d^2\sigma^{(i)}}{dQ dY} = \frac{\rho\pi\alpha_s^2}{2QS} \sum_{a,b,c,d} \frac{1}{1+\delta_{ab}} \frac{1}{1+\delta_{cd}} |\mathcal{M}_{abcd}^{(i)}|^2 \mathcal{L}_{ab}(\Delta y, Q) \Big|_{\Delta y=Y} \quad (3.22)$$

with

$$\mathcal{L}_{ab}(\Delta y, Q) = \frac{1}{2z} \int_{-\bar{y}^+}^{\bar{y}^+} d\bar{y} f_a(\sqrt{z}e^{\bar{y}/2}, Q) f_b(\sqrt{z}e^{-\bar{y}/2}, Q), \quad (3.23)$$

where $\bar{y} = y_3 + y_4$ and $\rho = \frac{4Q^2}{S}$. The integration limits are

$$\bar{y}^+ = \min \left(\ln \frac{1}{z}, \bar{y}_{\text{cut}} \right), \quad (3.24)$$

where the value \bar{y}_{cut} is obtained by requiring that both jets are within the calorimeter acceptance.

The resummation of global logarithms is achieved by considering the original four-parton matrix elements dressed by in-gap virtual gluons, with transverse momenta above Q_0 and no out-of-gap (real or virtual) gluons. The resummed partonic cross section then has the form

$$|\mathcal{M}^{(0)}|^2 = \text{tr} \left(H e^{-\xi(Q_0, Q) \mathbf{\Gamma}^\dagger} S e^{-\xi(Q_0, Q) \mathbf{\Gamma}} \right), \quad (3.25)$$

where ξ is computed by considering the strong coupling at one loop:

$$\xi(k_1, k_2) = \frac{2}{\pi} \int_{k_1}^{k_2} \frac{dk_T}{k_T} \alpha_s(k_T) = \frac{1}{\pi \beta_0} \ln \frac{1 + \alpha_s(Q) \beta_0 \ln \frac{k_2^2}{Q^2}}{1 + \alpha_s(Q) \beta_0 \ln \frac{k_1^2}{Q^2}}, \quad (3.26)$$

with $\beta_0 = \frac{11C_A - 2n_f}{12\pi}$. The matrix H in Eq. (3.25) gives the matrix elements of the hard process in some colour basis, while S is the metric tensor in that colour basis. In an orthonormal basis, as we use throughout this chapter, $S = 1$.

3.4.1 Non-global contribution

We want to estimate the impact of non-global logarithms on the gap fraction. In particular we aim to resum the non-global logarithms that arise as a result of allowing one soft gluon outside the rapidity gap. The general framework in which this calculation is performed is described in [91, 92], where the case of an azimuthally symmetric gap was considered. As in the global case this led to relatively simple analytical expressions. To include the gap definition used in the

ATLAS analysis instead, one has to resort to evaluating most of the integrals numerically. This considerably slows down the calculation, but has a very small effect on the final results. Therefore, for the current work, we decide to include non-global effects as a K -factor:

$$K(Q, \Delta y) = \frac{\frac{d^2\sigma^{(0)}}{dQ dY} + \frac{d^2\sigma^{(1)}}{dQ dY}}{\frac{d^2\sigma^{(0)}}{dQ dY}}, \quad (3.27)$$

where in calculating this ratio we compute the resummed cross sections for azimuthally symmetric gaps, and then use it to multiply the resummed result for zero gluons outside the gap including the exact gap definition. The error this approximation induces is much smaller than the overall uncertainty in the resummed approach, which we estimate below. This approximation does not affect our matching procedure because we are only performing LO matching and non-global logarithms start at $\mathcal{O}(\alpha_s^2)$ in the expansion of the gap fraction. We do not need to include effects related to parton recombination due to the particular choice of the jet-algorithm [96,97] since we employ the anti- k_t jet algorithm [84].

The calculation of the contribution from one gluon outside the gap is essentially that presented in [91,92], except that the final integral over that gluon's momentum is explicitly performed numerically: We briefly recap the results. To obtain the contribution from one gluon outside the gap we must consider both real and virtual corrections to the four-parton scattering, each dressed with any number of soft gluons:

$$|\mathcal{M}^{(1)}|^2 = -\frac{2}{\pi} \int_{Q_0}^Q \frac{dk_T}{k_T} \alpha_s(k_T) \int_{\text{out}} dy (\Omega_R + \Omega_V), \quad (3.28)$$

where the integrals are over the transverse momentum and rapidity of the real or virtual out-of-gap gluon. The operator to insert this gluon off the external legs is

$$\mathbf{D}^\mu = \mathbf{t}_a h_1^\mu + \mathbf{t}_b h_2^\mu + \mathbf{t}_c h_3^\mu + \mathbf{t}_d h_4^\mu,$$

$$h_i^\mu = \frac{1}{2} k_T \frac{p_i^\mu}{p_i \cdot k}, \quad (3.29)$$

for real emission, and

$$\begin{aligned} \gamma &= -\frac{1}{2} \left[\mathbf{t}_a \cdot \mathbf{t}_b \omega_{12} + \mathbf{t}_a \cdot \mathbf{t}_c \omega_{13} + \mathbf{t}_a \cdot \mathbf{t}_d \omega_{14} + \mathbf{t}_b \cdot \mathbf{t}_c \omega_{23} + \mathbf{t}_b \cdot \mathbf{t}_d \omega_{24} + \mathbf{t}_c \cdot \mathbf{t}_d \omega_{34} \right], \\ \omega_{ij} &= \frac{1}{2} k_T^2 \frac{p_i \cdot p_j}{p_i \cdot k p_j \cdot k}, \end{aligned} \quad (3.30)$$

for virtual emission. In the case of the out-of-gap gluon being virtual, the subsequent evolution is unchanged from that of the original four-parton system, given by $\mathbf{\Gamma}$ in Eq. (3.12). In the case of real emission we have to consider the colour evolution of a five-parton system [98,99]. If we assume the gluon to be emitted on the same side of the event as partons a and c , the anomalous dimension is given by

$$\begin{aligned} \mathbf{\Lambda} &= \frac{1}{2} Y \mathbf{T}_t^2 + i\pi \mathbf{T}_a \cdot \mathbf{T}_b + \frac{1}{4} \rho(Y; \Delta y) (\mathbf{T}_c^2 + \mathbf{T}_d^2) + \frac{1}{4} \rho(Y; 2|y|) \mathbf{T}_k^2 \\ &+ \frac{1}{2} \lambda(Y; |\Delta y|, |y|, \phi) \mathbf{T}_c \cdot \mathbf{T}_k, \end{aligned} \quad (3.31)$$

$$\mathbf{T}_t^2 = (\mathbf{T}_b + \mathbf{T}_d)^2 \quad (3.32)$$

and we have introduced the kinematic function

$$\lambda(Y; \Delta y, y, \phi) = \frac{1}{2} \ln \frac{\cosh(\Delta y/2 + y + Y) - \text{sgn}(y) \cos \phi}{\cosh(\Delta y/2 + y - Y) - \text{sgn}(y) \cos \phi} - Y. \quad (3.33)$$

The real and virtual out-of-gap emissions, dressed to all orders with in-gap virtual corrections are thus

$$\begin{aligned} \Omega_R &= \text{tr} \left[H e^{-\xi(k_T, Q) \mathbf{\Gamma}^\dagger} \mathbf{D}^{\mu\dagger} e^{-\xi(Q_0, k_T) \mathbf{\Lambda}^\dagger} e^{-\xi(Q_0, k_T) \mathbf{\Lambda}} \mathbf{D}_\mu e^{-\xi(k_T, Q) \mathbf{\Gamma}} \right], \\ \Omega_V &= \text{tr} \left[H e^{-\xi(Q_0, Q) \mathbf{\Gamma}^\dagger} e^{-\xi(Q_0, k_T) \mathbf{\Gamma}} \gamma e^{-\xi(k_T, Q) \mathbf{\Gamma}} + \text{c.c.} \right]. \end{aligned} \quad (3.34)$$

The K -factor defined in Eq. (3.27) is plotted in Fig. 3.5 as a function of Q for different Δy values and as a function of Δy for different values of Q . In the case

of the Q distribution, we see that the effect is modest for the first rapidity bin, but is typically of the order of 30% in much of the Q range we study.

It has been shown [91,92] that naïve QCD coherence is violated at sufficiently high perturbative orders because the Coulomb gluon exchange terms included in $\mathbf{\Gamma}$ and $\mathbf{\Lambda}$ induce a mis-cancellation between the real and virtual contributions in Eq. (3.28). The $y \rightarrow \infty$ region therefore gives a finite contribution and, as a consequence, super-leading logarithms ($\alpha_s^n \log^{n+1}(Q/Q_0)$) arise at $\mathcal{O}(\alpha_s^4)$ and beyond. The numerical impact of these contributions has been studied in [73] and found to be generally modest.

3.5 Matching

The resummed calculations are based on the eikonal approximation, in which energy-momentum is not conserved. There is no recoil of the hard lines against the emissions and no account of their effect on the incoming parton momentum fractions at which the parton distribution functions are evaluated. Matching to the full $2 \rightarrow 3$ matrix elements takes into account energy-momentum conservation, at least for the first (hardest) emission. Its energy is taken into account and it is hence less likely, so the matched gap fraction will be bigger than the one given in Eq. (3.21).

In this section we discuss the matching of the resummed gap fraction to the LO calculation. At LO we can write Eq. (3.19) as follows:

$$f_{LO}^{\text{gap}} = 1 - \frac{2\alpha_s(Q)}{\pi} \left[a_0(Q, Y) \ln \frac{Q}{Q_0} - b_0(Q, Q_0, Y) \right] + \mathcal{O}(\alpha_s^2), \quad (3.35)$$

where the contribution b_0 is now free of large logarithms of Q/Q_0 . We want to combine this expression with Eq. (3.21), subtracting the double counted term

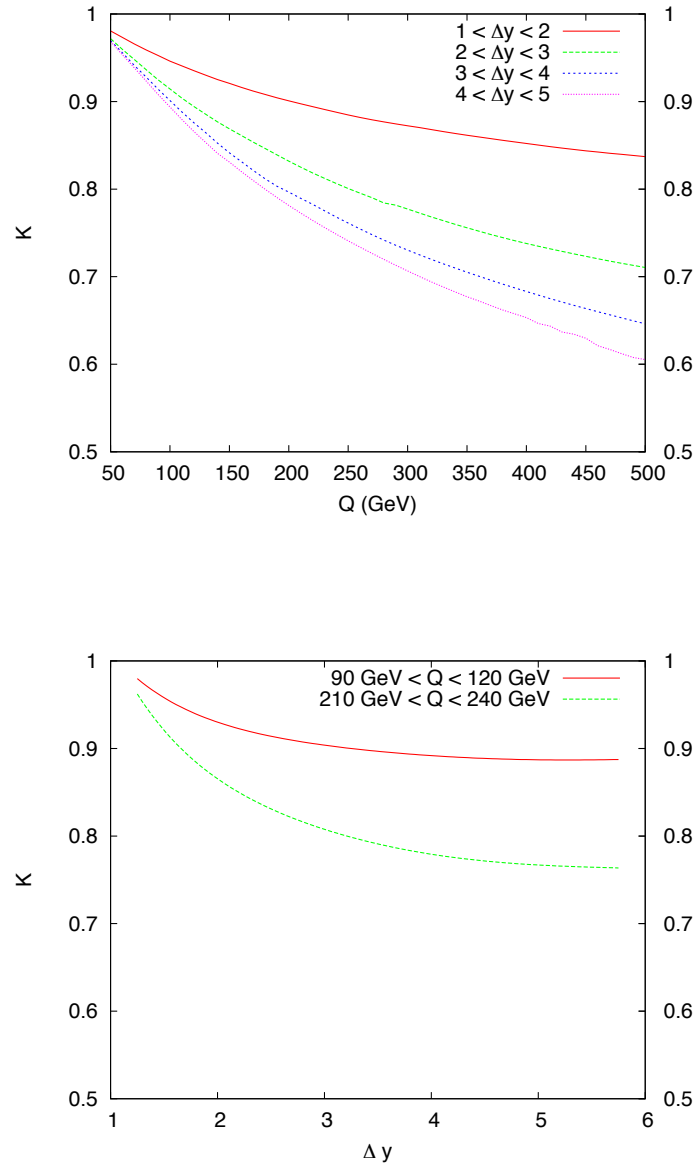


Figure 3.5: The K -factor we use to estimate non-global effects, as a function of Q for different values of Δy (above) and as a function of Δy , for different values of Q (below).

$1 - \frac{2\alpha_s}{\pi} a_0 \ln(Q/Q_0)$. Firstly, we have to verify that the two calculations agree in the asymptotic limit $\ln(Q/Q_0) \gg 1$. This can be easily achieved considering the logarithmic derivative of the gap fraction:

$$\frac{2\alpha_s(Q)}{\pi} a_0(Q, Y) = \lim_{Q_0 \rightarrow 0} \frac{d}{d \ln Q_0} f_{LO}^{\text{gap}} = - \lim_{Q_0 \rightarrow 0} \frac{d^3 \sigma^{\text{gap}}}{d \ln Q_0 dQ dY} / \frac{d^2 \sigma^{\text{born}}}{dQ dY}. \quad (3.36)$$

The result is shown in Fig. 3.6: the logarithmic derivative of the gap fraction is plotted as a function of $\ln(Q_0/Q)$ for fixed kinematics. In this particular example we have $\Delta y = 3$ and $Q = 200$ GeV. The plot shows that the logarithmic derivative of the gap fraction tends to a constant for large, and negative, values of the logarithm. The numerical value is in agreement with the one obtained by expanding the resummation at $\mathcal{O}(\alpha_s(Q))$:

$$\begin{aligned} f_{\text{res}}^{\text{gap}} &= 1 - a_0(Q, Y)\xi - a_1(Q, Y)\xi^2 + \dots \\ &= 1 - \frac{2\alpha_s(Q)}{\pi} a_0(Q, Y) \left[\ln \frac{Q}{Q_0} + \sum_{n=1}^{\infty} \beta_0^n \alpha_s(Q)^n \int_{Q_0}^Q \frac{dk_T}{k_T} \ln^n \frac{Q^2}{k_T^2} \right] + \mathcal{O}(\xi^2). \end{aligned} \quad (3.37)$$

The plot in Fig. 3.6 shows that we have control of the logarithms at $\mathcal{O}(\alpha_s)$. However, plotting instead the Q dependence at fixed Q_0 for various Δy bins, as in Fig. 3.7, the picture is not so clear. Because the plot is on a logarithmic x axis, we might naïvely expect the FO result (data points) to asymptotically tend to a straight line, with the same slope as the expansion of the resummation (dashed curve). However, changing the Q values, one changes the momentum fractions and factorization scales of the parton distribution functions and hence the mix of different flavour processes, so one could expect some curvature, but this effect should also be included in the expansion of the resummed results, where some curvature is also seen, so the differences in slope between the data points and

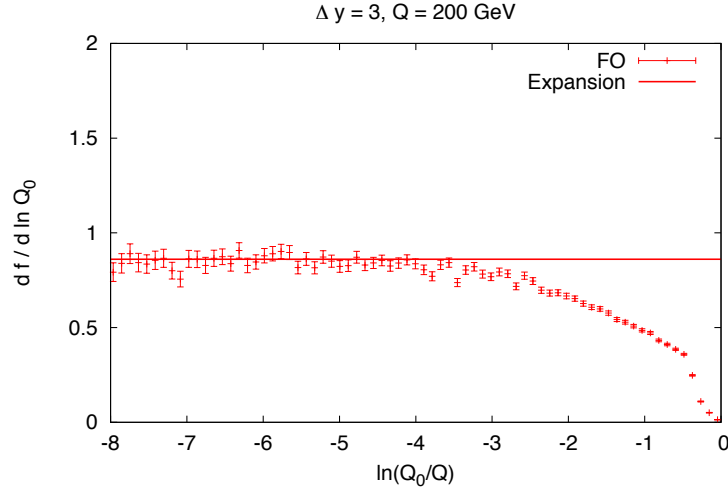


Figure 3.6: The logarithmic derivative of the gap fraction $\frac{df^{\text{gap}}}{d \ln Q_0}$ as a function of $\ln Q_0/Q$ for fixed $Q = 200$ GeV and $\Delta y = 3$ ($\sqrt{S} = 7$ TeV). The solid line is the coefficient obtained by expanding Eq. (3.21) at $\mathcal{O}(\alpha_s)$.

dashed curves is really significant. Because the FO curve and the expansion of the eikonal resummation differ so much, a simple matching procedure in which we add together the FO and the resummation and subtract their common term, is bound to fail. It is clear that this issue must be investigated in more detail. The strengthening of the curvature at the highest Q and Δy values indicates that we are becoming sensitive to the kinematic limit and we therefore examine the issue of energy-momentum conservation.

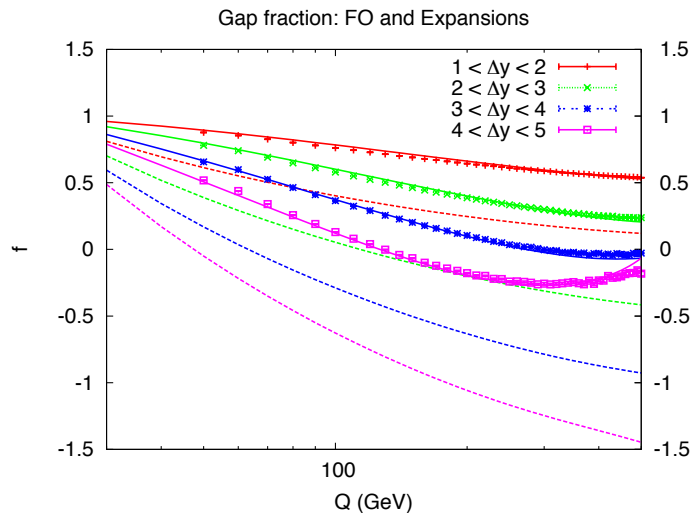


Figure 3.7: The gap fraction at $\mathcal{O}(\alpha_s)$ as a function of Q in different Δy bins. The points are the exact FO calculations, the dashed curves the expansions of the eikonal resummation (Eq. (3.37)) and the solid curves correspond to the $\mathcal{O}(\alpha_s)$ expansion of the modified resummation.

3.5.1 Energy-momentum conservation

The resummed cross section (Eq. (3.22)) has been obtained in the eikonal limit, i.e. emitted gluons are considered soft and they do not change the Born kinematics. Even if we are guaranteed that this assumption is sufficient to capture the leading logarithmic behaviour, we are losing important physical effects related to energy-momentum conservation. In particular, because of the choice $Q_0 = 20$ GeV we are sensitive to emissions of gluons with non-negligible transverse momentum with respect to Q . Furthermore, the emission of a gluon requires a finite amount of energy and, for given Q and Δy , this means we are probing the parton distribution

functions at larger values of $x_{1,2}$. Because the PDFs are steeply falling functions of x at large x this can give a considerable suppression well before we reach the edge of phase space.

We would therefore like to go beyond the soft approximation and modify our resummation so that we can capture the correct kinematic behaviour, at least for the hardest (i.e. highest k_T) gluon emission. In order to do that we study the full kinematics of a $2 \rightarrow 3$ process and using energy-momentum conservation we determine the values of $x_{1,2}$:

$$x_{1,2} = A_{\pm} e^{\pm \bar{y}}, \quad \text{with} \quad A_{\pm} = \frac{2}{\sqrt{S}} \left[Q \cosh \frac{\Delta y}{2} \pm \bar{Q} \sinh \frac{\Delta y}{2} + \frac{k_T}{2} e^{\pm y'} \right]. \quad (3.38)$$

We see that $x_{1,2}$ depend on the transverse momentum of the emitted gluon k_T and its rapidity in the partonic centre of mass frame, y' . We have also introduced

$$\bar{Q} = p_{T3} - p_{T4} = -\frac{k_T k_T + 2Q \cos \phi}{2 \cdot 2Q + k_T \cos \phi}. \quad (3.39)$$

As a consequence the parton luminosities become

$$\tilde{\mathcal{L}}_{ab}(\Delta y, Q, k) = \frac{1}{2A_+ A_-} \int_{\bar{y}^-}^{\bar{y}^+} d\bar{y} f_a(A_+ e^{\bar{y}/2}, Q) f_b(A_- e^{-\bar{y}/2}, Q), \quad (3.40)$$

with

$$\begin{aligned} \bar{y}^- &= \max(\ln A_-^2, -\bar{y}_{\text{cut}}), \\ \bar{y}^+ &= \min\left(\ln \frac{1}{A_+^2}, \bar{y}_{\text{cut}}\right). \end{aligned} \quad (3.41)$$

If we take the limit $k_T \rightarrow 0$ then Eq. (3.40) reduces to the parton luminosity computed in the soft limit, Eq. (3.23).

So far we have discussed how to take into account the complete kinematics in the PDFs for the hardest emission. Clearly, the matrix elements will also differ

from their eikonal approximations and the gap fraction ($f = 1 - d\sigma^{\text{gap}}/d\sigma^{\text{born}}$) involves

$$\frac{d\sigma^{\text{gap}}}{dQdY} = \int dk_T dy' d\phi |\mathcal{M}_{2\rightarrow 3}(\Delta y, Q, k)|^2 \tilde{\mathcal{L}}(\Delta y, Q, k), \quad (3.42)$$

where we have suppressed parton indices for clarity. Since both the matrix elements and the parton luminosities depend on the momentum of the emitted parton, k , we lose the convenient kinematic factorization of Eq. (3.22). Importantly, it is the shift in the argument of the PDFs that dominates, and so we shall evaluate the matrix elements in the eikonal limit. To further simplify matters we can also restore the kinematic factorization by approximating the integral of the parton luminosity by its value at a particular phase space point. Specifically, we write

$$\frac{d\sigma^{\text{gap}}}{dQdY} \approx \int dk_T dy' d\phi |\mathcal{M}_{2\rightarrow 3}(\Delta y, Q, k)|_{\text{soft}}^2 \tilde{\mathcal{L}}(\Delta y, Q, k) \Big|_{k_T=\sqrt{Q_0 Q}, y'=\alpha\Delta y} \quad (3.43)$$

and the value of \bar{Q} is determined by its azimuthal average:

$$\int_0^{2\pi} \frac{d\phi}{2\pi} \bar{Q} = -\frac{k_T^2}{8Q} + \mathcal{O}(k_T^4). \quad (3.44)$$

For the transverse momentum, we have chosen the geometric mean of the integration limits, i.e. $k_T = \sqrt{Q_0 Q}$. The rapidity value is determined by requiring the approximate result on the right hand side of (3.43) to be as close as possible to its exact value on the left hand side. We keep α fixed as we vary Q , but allow it to vary with Δy and typically find $\frac{1}{4} \lesssim \alpha \lesssim \frac{1}{3}$.

The $\mathcal{O}(\alpha_s)$ modified gap fraction is plotted in Fig. 3.7 with solid lines. The plot shows that with a one parameter fit we can construct a modified resummation whose first-order expansion reproduces the FO result very accurately. We stress that this modification of the parton luminosity does not affect the formal leading logarithmic accuracy of our calculation. Rather it corresponds to a particular choice of important sub-leading terms that is motivated by energy-momentum

conservation: it is very reassuring that such a procedure reproduces so well the exact leading order result.

Using this modified resummed result we are now ready to complete the matching to LO (the matching corrections are now very small), estimate the theoretical uncertainty and then compare to data.

3.6 Matched results and comparison to data

We define our modified resummed cross section (for zero gluons outside the gap), i.e. the replacement of Eq. (3.22), as

$$\begin{aligned} \frac{d^2\sigma^{\text{mod}}}{dQ dY} &= \frac{\rho\pi\alpha_s^2}{2QS} \sum_{a,b,c,d} \frac{1}{1+\delta_{ab}} \frac{1}{1+\delta_{cd}} \left\{ |\mathcal{M}_{abcd}^{\text{born}}|^2 \mathcal{L}_{ab}(\Delta y, Q^2) + \left(|\mathcal{M}_{abcd}^{(0)}|^2 - |\mathcal{M}_{abcd}^{\text{born}}|^2 \right) \right. \\ &\quad \left. \times \tilde{\mathcal{L}}_{ab}(\Delta y, Q, k) \Big|_{k_T=\sqrt{Q_0}Q, y'=\alpha\Delta y} \right\}. \end{aligned} \quad (3.45)$$

We then define a resummed gap fraction by adding the FO calculation and the modified resummation together, subtracting the expansion of the resummed expression to $\mathcal{O}(\alpha_s)$:

$$f_{\text{matched}}^{\text{gap}} = f_{LO}^{\text{gap}} + f_{\text{mod}}^{\text{gap}} - f_{\text{mod},\alpha_s}^{\text{gap}}. \quad (3.46)$$

We also estimate the effects of non-global logarithms by multiplying the above expression by the K -factor defined in Eq. (3.27). The calculation we have performed matches together a LO computation with a leading logarithmic one and so we expect it to have a considerable theoretical uncertainty. Because we are considering the gap fraction, renormalisation and factorization scale variations do not give the dominant contribution to the uncertainty. Parton-distribution-function effects also largely cancel in the ratio. The dominant source of uncertainty comes from higher logarithmic orders in the resummation. In particular, a leading logarithmic

resummation does not fix the argument of the logarithms we are resumming. As an estimate of our theoretical uncertainty we then rescale the argument of the function ξ , Eq. (3.26):

$$\xi(Q_0, Q) \longrightarrow \xi(\gamma Q_0, Q), \quad (3.47)$$

with γ allowed to vary in a range of order unity. Motivated by the fact that next-to-leading logarithmic corrections to leading soft logarithms are typically found to be negative, we consider variations in the upward direction by, quite arbitrarily, a factor of 2, i.e. $1 < \gamma < 2$.

The plots in Fig. 3.8 show the gap fraction as a function of the mean transverse momentum of the two leading jets Q in four different rapidity bins, while the ones in Fig. 3.9 are for the Δy distribution, in two different Q bins. We use the same cuts as the ATLAS analysis: all jets must have $p_T > 20$ GeV, $|y| < 4.4$ and the mean transverse momentum of the two highest transverse momentum jets must be $Q > 50$ GeV. The dash-dotted red line represents the LO calculation, the dashed green line the resummed gap fraction in the eikonal limit, solid blue is the resummed and matched result Eq. (3.46), with the band obtained by varying γ , as explained above, and finally the magenta band corresponds to the resummed and matched gap fraction with the non-global effects included. The black crosses are the data points measured by the ATLAS collaboration [52] with the gap defined by the two highest p_T jets (we have combined the statistical and systematic errors in quadrature).

The FO calculation is clearly only sensible in the first rapidity bin and for $\Delta y > 2$ it decreases very rapidly as a function of Q and eventually becomes negative. This unphysical behaviour is driven by a large logarithmic term $\sim \alpha_s \Delta y \ln \frac{Q}{Q_0}$ which needs to be resummed. The eikonal resummation restores the

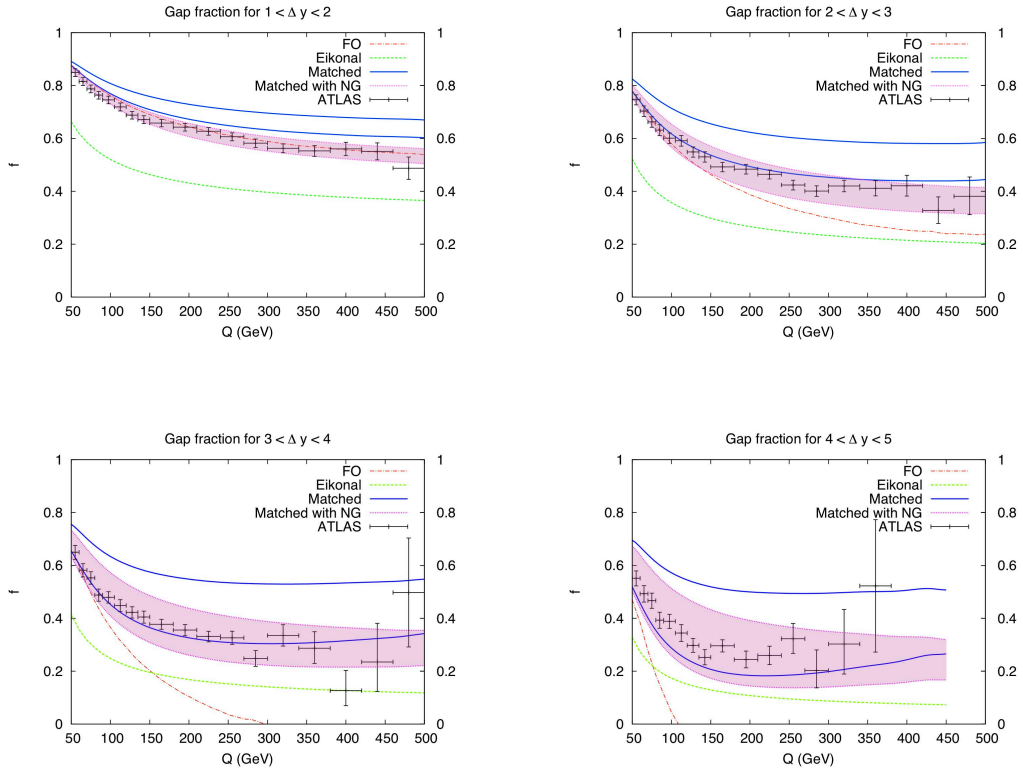


Figure 3.8: The fixed order prediction, the eikonal resummation at all orders, and the matched gap fraction as a function of the transverse momentum Q in different rapidity bins.

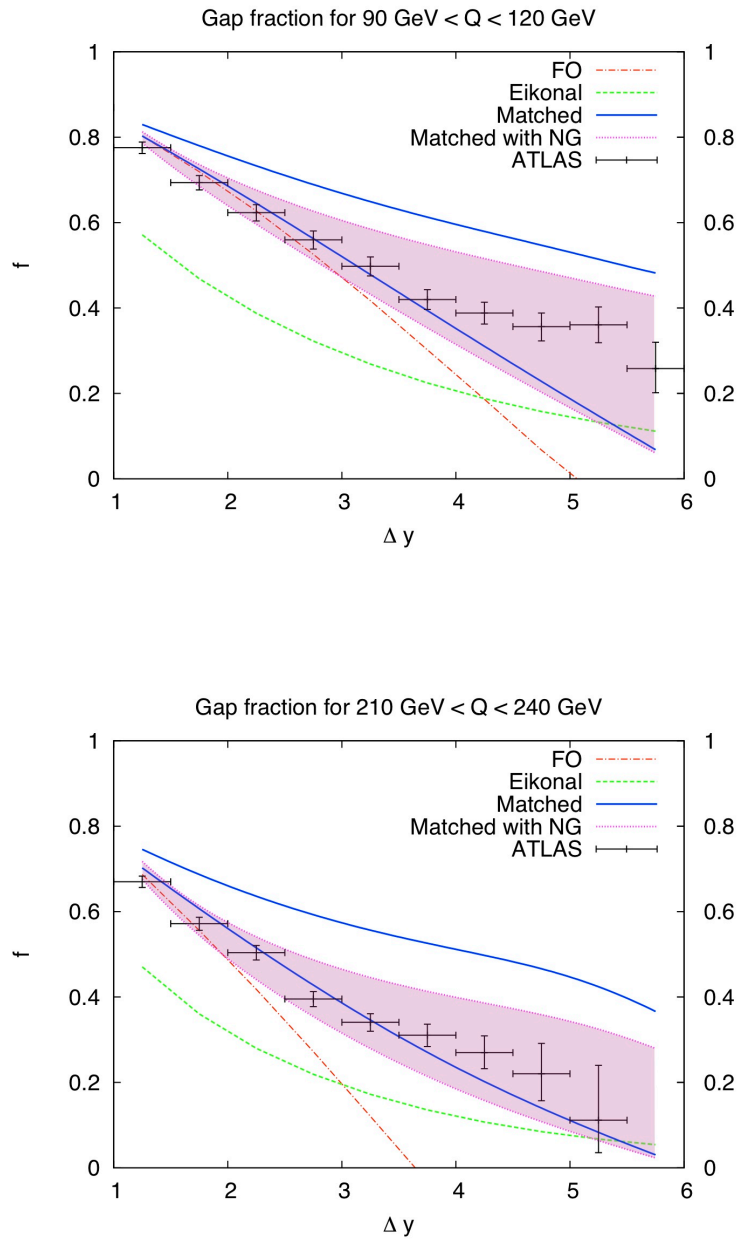


Figure 3.9: The matched gap fraction as a function of rapidity separation Δy in two different transverse momentum bins.

physical behaviour but, as we have previously discussed, completely ignores the issue of energy-momentum conservation and produces too small a gap fraction. Our matched curves, with the inclusion of non-global logarithms, does seem to capture most of the salient physics. However, our results are affected by large theoretical uncertainties due to the fact the calculation is accurate only at the leading logarithmic level. The extension of resummation for the gap cross section at the next-to-leading logarithmic accuracy will certainly reduce this uncertainty but it is not an easy task and it is not likely that it is going to be completed soon. Another way of reducing the uncertainty is to perform the matching at NLO, so that any dependency on the rescaling factor γ is pushed one order higher in the strong coupling. With the necessary NLO calculations available in NLOJET++ [83], such a NLO matching is certainly feasible.

3.7 Discussion and conclusions

In Ref. [52] comparisons are made between the data and the predictions of some of the different theoretical tools currently available. Firstly we notice that gap fractions are defined there with respect to the dijet cross section at NLO, while we use the Born cross section. We have checked that, because of the definition of Q as the mean transverse momentum, NLO corrections are small. The best description of the data was found using POWHEG [100–102], interfaced with PYTHIA [103]. The results obtained using POWHEG interfaced with HERWIG++ [16] were found to undershoot the data. The difference between the two parton showers can be taken as indicative of the theoretical uncertainty due to the parton shower–NLO matching. The formal accuracy of the POWHEG calculations appearing in the ATLAS paper is not different to ours: tree-level matrix elements are used and then

matched to a parton shower, which is essentially a leading logarithmic resummation. However, the final predictions differ from ours because of the assumptions and approximations contained in the showering algorithm. Firstly, energy-momentum conservation is properly accounted for in every emission in a parton shower, not just the hardest as in our calculation. Also, the parton shower is limited to the large N_c approximation, but it does include non-global logarithms beyond the “one out-of-gap gluon approximation”. Another effect which is missing in the parton shower approach is Coulomb gluon exchange. As pointed out in [73] these contributions are especially important in the large Q/Q_0 and large Δy region: Coulomb gluons contribute to building up the colour-singlet exchange contribution, which eventually leads to a rise of the gap fraction at large enough Δy .

The ATLAS collaboration also compared their data to theoretical predictions obtained with HEJ [86]. That framework is based on the factorization of multi-gluon amplitudes in the high-energy regime. As in the BFKL approach, $\alpha_s^n \Delta y^n$ terms are resummed, but energy-momentum conservation is enforced. Logarithms of Q/Q_0 are not systematically resummed, unless they come with a Δy factor. We notice that the HEJ predictions are similar to ours for the global part, after accounting for energy-momentum conservation. This does not come as a surprise: Although the two approaches resum different terms, the leading contributions are of the form $\alpha_s^n \Delta y^n \ln^n \frac{Q}{Q_0}$ and are resummed in both approaches. HEJ describes emissions of out-of-gap gluons and, if interfaced with a parton shower, should be capable of capturing non-global logarithms as well [104]. We note that the HEJ framework does not at present include colour mixing via Coulomb gluons.

It seems clear that within the context of the overall accuracy of a leading log/leading order matching and the kinematic range of the current data, the impact

of sub-leading N_c and Coulomb gluon effects is not yet critical (except perhaps at the largest values of Δy where both PYTHIA and HERWIG++ undershoot the data). The same cannot be said about the constraints of energy-momentum conservation, which are clearly very important. The message is clear: the accuracy of the ATLAS data already demands better theoretical calculations.

Closing remarks

In this thesis we have computed the resummation of logarithmic terms arising from the emission of soft gluons for two different scattering processes: Z-boson production and gaps between jets.

Our study on Z-boson production was motivated by the recent proposal of a novel variable a_T [9] which improves the experimental accuracy at the low p_T region and thus helps to constraint non-perturbative effects. The resummation has been recently improved to better accuracy in Ref. [46]. The studies on a_T have further motivated the proposal of a similar observable ϕ^* [?, 47]; its resummation matched to fixed-order predictions has been compared to data in Ref. [48].

On the other hand, we have also studied gaps between jets and compared our results with the data measured by the ATLAS collaboration [52]. We have calculated the resummation of soft gluons coming from mismatched virtuals in the veto and have matched this result to a fixed order prediction, including a correction to the eikonal result to account for energy-momentum conservation in the process. We have also studied the impact of having one gluon emitted outside the gap and have improved thus the study of colour-singlet exchanged events at hadron colliders. In the future, we can look forward to data on W or Z + dijets and vetoing in that case, as a precursor to Higgs + dijets. We can also look forward

to NLO matching and to further studies of the non-global logarithms computed in terms of the expansion in number of out-of-gap gluons. A big challenge for the future, which impacts the a_T and low p_T studies too, is to incorporate non-diagonal colour effects into a Monte Carlo.

Bibliography

- [1] Michael E. Peskin and Daniel V. Schroeder *An Introduction to Quantum Field Theory (Frontiers in Physics)*
- [2] R. K. Ellis, W. J. Stirling and B. R. Webber, *QCD and collider physics, Camb. Monogr. Part. Phys. Nucl. Phys. Cosmol.* **8** (1996) 1.
- [3] L. N. Lipatov, *Sov. J. Nucl. Phys.* **20** (1975) 95.
- [4] V. N. Gribov and L. N. Lipatov, *Sov. J. Nucl. Phys.* **15** (1972) 438.
- [5] G. Altarelli and G. Parisi, *Nucl. Phys.* **B126** (1977) 298.
- [6] Yu. L. Dokshitzer, *Sov. Phys. JETP* **46** (1977) 641.
- [7] J. C. Collins and D. E. Soper *Ann. Rev. Nucl. Part. Sci.* **37** (1987) 221.
- [8] J. C. Collins, D. E. Soper and G. Sterman, *Soft Gluons and Factorization, Nucl. Phys.* **B 308** (1988) 833.
- [9] M. Vesterinen and T. R. Wyatt, *A Novel Technique for Studying the Z Boson Transverse Momentum Distribution at Hadron Colliders, Nucl. Instrum. Meth.* **A 602** (2009) 432, [arXiv:0807.4956].
- [10] W.J. Stirling and M.R. Whalley, *A Compilation of Drell-Yan cross-sections, J. Phys.* **G 19** (1993) D1.
- [11] A. A. Affolder *et al.* [CDF Collaboration], *The transverse momentum and total cross section of e^+e^- pairs in the Z boson region from $p\bar{p}$ collisions at $\sqrt{s} = 1.8$ TeV, Phys. Rev. Lett.* **84** (2000) 845 [hep-ex/0001021].
- [12] B. Abbot *et al.* [D0 Collaboration], *Measurement of the inclusive differential cross section for Z bosons as a function of transverse momentum in $p\bar{p}$ collisions at $\sqrt{s} = 1.8$ TeV, Phys. Rev.* **D 61** (2000) 032004 [hep-ex/9907009].

- [13] C. T. H. Davies, B. R. Webber and W. J. Stirling, *Drell-Yan Cross-Sections At Small Transverse Momentum*, *Nucl. Phys.* **B 256** (1985) 413.
- [14] G. Bozzi, S. Catani, G. Ferrera, D. de Florian and M. Grazzini, *Transverse-momentum resummation: a perturbative study of Z production at the Tevatron*, *Nucl. Phys.* **B 815** (2009) 174 [arXiv:0812.2862].
- [15] F. Landry, R. Brock, P. M. Nadolsky and C. P. Yuan, *Tevatron Run-1 Z boson data and Collins-Soper-Sterman resummation formalism*, *Phys. Rev.* **D 67** (2003) 073016 [hep-ph/0212159].
- [16] M. Bahr *et al.*, *Herwig++ Physics and Manual*, *Eur. Phys. J.* **C 58** (2008) 639 [arXiv:0803.0883].
- [17] S. Gieseke, M. H. Seymour and A. Siodmok, *A Model of non-perturbative gluon emission in an initial state parton shower*, *J. High Energy Phys.* **06** (2008) 001 [arXiv:0712.1199].
- [18] S. Berge, P. M. Nadolsky, F. Olness and C. P. Yuan, *Transverse momentum resummation at small x for the Tevatron and CERN LHC*, *Phys. Rev.* **D 72** (2005) 033015 [hep-ph/0410375].
- [19] M. Dasgupta and Y. Delenda, *The Q_t distribution of the Breit current hemisphere in DIS as a probe of small-x broadening effects*, *J. High Energy Phys.* **08** (2006) 080 [hep-ph/0606285].
- [20] D0 Collaboration *Phys. Rev. Lett.* **100** (2008) 102002.
- [21] C. Bálazs and C. P. Yuan, *Soft gluon effects on lepton pairs at hadron colliders*, *Phys. Rev.* **D 56** (1997) 5558 [hep-ph/9704258].
- [22] Yu. L. Dokshitzer, D. Diakonov and S. I. Troyan, *On The Transverse Momentum Distribution Of Massive Lepton Pairs*, *Phys. Lett.* **B 79** (1978) 269.
- [23] G. Altarelli, G. Parisi and R. Petronzio, *Transverse Momentum Of Muon Pairs Produced In Hadronic Collisions*, *Phys. Lett.* **B 76** (1978) 356.
- [24] J. C. Collins, D. E. Soper and G. Sterman, *Transverse Momentum Distribution In Drell-Yan Pair And W And Z Boson Production*, *Nucl. Phys.* **B 250** (1985) 199.
- [25] R. K. Ellis, D. A. Ross and S. Veseli, *Vector boson production in hadronic collisions*, *Nucl. Phys.* **B 503** (1997) 309 [hep-ph/9704239].
- [26] R. K. Ellis and S. Veseli, *W and Z transverse momentum distributions: Resummation in q_T -space*, *Nucl. Phys.* **B 511** (1998) 649 [hep-ph/9706526].

- [27] S. Catani, D. de Florian and M. Grazzini, *Universality of non-leading logarithmic contributions in transverse momentum distributions*, *Nucl. Phys.* **B 596** (2001) 299 [[hep-ph/0008184](#)]. D. de Florian and M. Grazzini, *Next-to-next-to-leading logarithmic corrections at small transverse momentum in hadronic collisions*, *Phys. Rev. Lett.* **85** (2000) 4678 [[hep-ph/0008152](#)].
- [28] A. Banfi, M. Dasgupta, R. M. Duran Delgado *JHEP* **0912** (2009) 022 [[hep-ph/0909.5327](#)].
- [29] Andreas Papaefstathiou, Jennifer M. Smillie, Bryan R. Webber *JHEP* **1004** (2010) 084 [[hep-ph/1002.4375](#)].
- [30] A. Banfi, M. Dasgupta and Y. Delenda, *Azimuthal decorrelations between QCD jets at all orders*, *Phys. Lett.* **B 665** (2008) 86 [[arXiv:0804.3786](#)].
- [31] J. Campbell, R.K. Ellis, *Next-to-leading order corrections to $W + 2$ jet and $Z + 2$ jet production at hadron colliders*, *Phys. Rev.* **D 65** (2002) 113007, <http://mcfm.fnal.gov/> [[hep-ph/0202176](#)].
- [32] A. Banfi and M. Dasgupta, *Dijet rates with symmetric E_t cuts*, *J. High Energy Phys.* **01** (2004) 027 [[hep-ph/0312108](#)].
- [33] P. Aurenche and J. Lindfors, *QCD Corrections To Direct Lepton Production In Hadronic Collisions*, *Nucl. Phys.* **B 185** (1981) 274.
- [34] G. Altarelli, R. K. Ellis and G. Martinelli, *Leptoproduction and Drell-Yan processes beyond the leading approximation in Chromodynamics*, *Nucl. Phys.* **B 143** (1978) 521 [Erratum *ibid.* **B 146** (1978) 544].
- [35] D. de Florian and M. Grazzini, *The structure of large logarithmic corrections at small transverse momentum in hadronic collisions*, *Nucl. Phys.* **B 616** (2001) 247. [[hep-ph/0108273](#)].
- [36] J. Pumplin, D. R. Stump, J. Huston, H. L. Lai, P. M. Nadolsky and W. K. Tung, *New generation of parton distributions with uncertainties from global QCD analysis*, *J. High Energy Phys.* **07** (2002) 012 [[hep-ph/0201195](#)].
- [37] A. Banfi, G. P. Salam and G. Zanderighi, *Principles of general final-state resummation and automated implementation*, *J. High Energy Phys.* **0503** (2005) 073 [[hep-ph/0407286](#)].
- [38] M. Dasgupta and G. P. Salam, *Resummation of non-global QCD observables*, *Phys. Lett.* **B 512** (2001) 323 [[hep-ph/0104277](#)].
- [39] M. Dasgupta and G. P. Salam, *Accounting for coherence in interjet E_t flow: A case study*, *J. High Energy Phys.* **03** (2002) 017 [[hep-ph/0203009](#)].

- [40] S. Catani, B. R. Webber and G. Marchesini, *QCD coherent branching and semiinclusive processes at large x*, *Nucl. Phys.* **B 349** (1991) 635.
- [41] A. Banfi, G. Marchesini and G. Smye, *Azimuthal correlation in DIS*, *J. High Energy Phys.* **04** (2002) 024 [[hep-ph/0203150](#)].
- [42] V. Antonelli, M. Dasgupta and G. P. Salam, *Resummation of thrust distributions in DIS*, *J. High Energy Phys.* **02** (2000) 001 [[hep-ph/9912488](#)].
- [43] S. Catani, L. Trentadue, G. Turnock and B. R. Webber, *Resummation of large logarithms in e^+e^- event shape distributions*, *Nucl. Phys.* **B 407** (1993) 3.
- [44] Y. L. Dokshitzer, G. Marchesini and B. R. Webber, *Non-perturbative effects in the energy-energy correlation*, *J. High Energy Phys.* **07** (1999) 012 [[hep-ph/9905339](#)].
- [45] A. Guffanti and G. E. Smye, *Nonperturbative effects in the W and Z transverse momentum distribution*, *J. High Energy Phys.* **10** (2000) 025 [[hep-ph/9905339](#)].
- [46] A. Banfi, M. Dasgupta, S. Marzani *QCD predictions for new variables to study dilepton transverse momenta at hadron colliders* *Phys. Lett.* **B 701** (2011) 75 [[hep-ph/1102.3594](#)].
- [47] A. Banfi, S. Redford, M. Vesterinen, P. Waller and T. R. Wyatt *Optimisation of variables for studying dilepton transverse momentum distributions at hadron colliders* *Eur.Phys.J.* **C71** (2011) 1600 [[hep-ex/1009.1580](#)].
- [48] S. Marzani, A. Banfi, M. Dasgupta and L. Tomlinson *Accurate QCD predictions for new variables to study dilepton transverse momentum* [[hep-ph/1106.6294](#)].
- [49] V. M. Abazov et al. [D0 Collaboration], *Precise study of the Z/gamma* boson transverse momentum distribution in ppbar collisions using a novel technique* *Phys. Rev. Lett.* **106** (2011) 122001 [[hep-ex/1010.0262](#)].
- [50] G. Aad et al. [ATLAS Collaboration], *Measurement of inclusive jet and dijet cross sections in proton-proton collisions at 7 TeV centre-of-mass energy with the ATLAS detector*, *Eur. Phys. J.* **C71** (2011) 1512. [[hep-ex/1009.5908](#)].
- [51] G. Aad et al. [ATLAS Collaboration], *Measurement of Dijet Azimuthal Decorrelations in pp Collisions at $\sqrt{s}=7$ TeV*, *Phys. Rev. Lett.* **106**, 172002 (2011). [[hep-ex/1102.2696](#)].

- [52] G. Aad *et al.* [ATLAS Collaboration], *Measurement of dijet production with a veto on additional central jet activity in pp collisions at $\sqrt{s}=7$ TeV using the ATLAS detector* [[hep-ex/1107.1641](#)].
- [53] S. Chatrchyan *et al.* [CMS Collaboration], *Measurement of the Ratio of the 3-jet to 2-jet Cross Sections in pp Collisions at $\sqrt{s} = 7$ TeV*, [[hep-ex/1106.0647](#)].
- [54] S. Chatrchyan *et al.* [CMS Collaboration], *Measurement of the Inclusive Jet Cross Section in pp Collisions at $\sqrt{s} = 7$ TeV*, [[hep-ex/1106.0208](#)].
- [55] S. Chatrchyan *et al.* [CMS Collaboration], *Measurement of the differential dijet production cross section in proton-proton collisions at $\sqrt{s}=7$ TeV*, Phys. Lett. **B700** (2011) 187-206. [[hep-ex/1104.1693](#)].
- [56] V. Khachatryan *et al.* [CMS Collaboration], *Dijet Azimuthal Decorrelations in pp Collisions at $\sqrt{s} = 7$ TeV*, Phys. Rev. Lett. **106** (2011) 122003. [[hep-ex/1101.5029](#)].
- [57] A. Buckley *et al.*, *General-purpose event generators for LHC physics*, [[hep-ph/1101.2599](#)]. To appear in Physics Reports.
- [58] A. Kulesza and L. Motyka, *Threshold resummation for squark-antisquark and gluino-pair production at the LHC*, Phys. Rev. Lett. **102** (2009) 111802 [[hep-ph/0807.2405](#)].
- [59] A. Kulesza and L. Motyka, *Soft gluon resummation for the production of gluino-gluino and squark-antisquark pairs at the LHC*, Phys. Rev. D **80** (2009) 095004 [[hep-ph/0905.4749](#)].
- [60] I. Sung, *Probing the Gauge Content of Heavy Resonances with Soft Radiation*, Phys. Rev. D **80** (2009) 094020 [[hep-ph/0908.3688](#)].
- [61] B. E. Cox, J. R. Forshaw, A. D. Pilkington, *Extracting Higgs boson couplings using a jet veto*, Phys. Lett. **B696** (2011) 87-91. [[hep-ph/1006.0986](#)].
- [62] Y. L. Dokshitzer, V. A. Khoze, T. Sjöstrand, *Rapidity gaps in Higgs production*, Phys. Lett. **B274** (1992) 116-121.
- [63] J. Keates, University of Manchester PhD thesis, 2009.
- [64] B. Abbott *et al.* [D0 Collaboration], *Probing hard color-singlet exchange in $p\bar{p}$ collisions at $\sqrt{s} = 630$ GeV and 1800 GeV*, Phys. Lett. B **440** (1998) 189 [[hep-ex/9809016](#)].

- [65] F. Abe *et al.* [CDF Collaboration], *Dijet production by color-singlet exchange at the Fermilab Tevatron*, Phys. Rev. Lett. **80** (1998) 1156; *ibid.* Phys. Rev. Lett. **81** (1998) 5278.
- [66] M. Derrick *et al.* [ZEUS Collaboration], *Rapidity Gaps between Jets in Photoproduction at HERA*, Phys. Lett. B **369** (1996) 55 [[hep-ex/9510012](#)].
- [67] S. Chekanov *et al.* [ZEUS Collaboration], *Photoproduction of events with rapidity gaps between jets at HERA*, [hep-ex/0612008](#)].
- [68] C. Adloff *et al.* [H1 Collaboration], *Energy flow and rapidity gaps between jets in photoproduction at HERA*, Eur. Phys. J. C **24** (2002) 517 [[hep-ex/0203011](#)].
- [69] V. D. Barger, R. J. N. Phillips and D. Zeppenfeld, *Mini - jet veto: A Tool for the heavy Higgs search at the LHC*, Phys. Lett. B **346** (1995) 106 [[hep-ph/9412276](#)].
- [70] N. Kauer, T. Plehn, D. L. Rainwater and D. Zeppenfeld, *H to W W as the discovery mode for a light Higgs boson*, Phys. Lett. B **503** (2001) 113 [[hep-ph/0012351](#)].
- [71] D. L. Rainwater *Searching for the Higgs boson* [[hep-ph/0702124](#)].
- [72] J. R. Forshaw and M. Sjö Dahl, *Soft gluons in Higgs plus two jet production*, JHEP **0709** (2007) 119 [[hep-ph/0705.1504](#)].
- [73] J. Forshaw, J. Keates and S. Marzani, *Jet vetoing at the LHC*, JHEP **0907** (2009) 023 [[hep-ph/0905.1350](#)].
- [74] A. Schofield and M. H. Seymour, *Jet vetoing and Herwig++*, [hep-ph/1103.4811](#).
- [75] R. M. Duran Delgado, J. R. Forshaw, S. Marzani and M. H. Seymour. *The dijet cross section with a jet veto* JHEP **1108** (2011) 157 [[hep-ph/1107.2084](#)].
- [76] S. Catani, M. Ciafaloni and G. Marchesini, *Noncancelling Infrared Divergences In QCD Coherent State*, Nucl. Phys. B **264** (1986) 588.
- [77] S. Catani and M. H. Seymour, *The Dipole Formalism for the Calculation of QCD Jet Cross Sections at Next-to-Leading Order*, Phys. Lett. B **378** (1996) 287 [[hep-ph/9602277](#)].
- [78] S. Catani and M. H. Seymour, *A general algorithm for calculating jet cross sections in NLO QCD*, Nucl. Phys. B **485** (1997) 291 [Erratum-*ibid.* B **510** (1998) 503] [[hep-ph/9605323](#)].

- [79] Yu. L. Dokshitzer and G. Marchesini, *Soft gluons at large angles in hadron collisions*, JHEP **0601** (2006) 007 [[hep-ph/0509078](#)].
- [80] Yu. L. Dokshitzer and G. Marchesini, *Hadron collisions and the fifth form factor*, Phys. Lett. B **631** (2005) 118 [[hep-ph/0508130](#)].
- [81] F. Bloch and A. Nordsieck, Phys. Rev. **52** (1937) 54.
- [82] R. B. Appleby and M. H. Seymour, *The Resummation of interjet energy flow for gaps between jets processes at HERA*, JHEP **0309** (2003) 056 [[hep-ph/0308086](#)].
- [83] Z. Nagy, *Next-to-leading order calculation of three jet observables in hadron hadron collision*, Phys. Rev. D **68** (2003) 094002 [[hep-ph/0307268](#)].
- [84] M. Cacciari, G. P. Salam and G. Soyez, *The Anti-k(t) jet clustering algorithm*, JHEP **0804** (2008) 063 [[hep-ph/0802.1189](#)].
- [85] P. M. Nadolsky *et al.*, *Implications of CTEQ global analysis for collider observables*, Phys. Rev. D **78** (2008) 013004 [[hep-ph/0802.0007](#)].
- [86] J. R. Andersen and J. M. Smillie, *Multiple Jets at the LHC with High Energy Jets*, JHEP **1106** (2011) 010 [[hep-ph/1101.5394](#)].
- [87] J. R. Forshaw, A. Kyrieleis, M. H. Seymour, *Gaps between jets in the high energy limit*, JHEP **0506** (2005) 034. [[hep-ph/0502086](#)].
- [88] N. Kidonakis, G. Oderda and G. Sterman, *Evolution of color exchange in QCD hard scattering*, Nucl. Phys. B **531** (1998) 365 [[hep-ph/9803241](#)].
- [89] G. Oderda and G. Sterman, *Energy and color flow in dijet rapidity gaps*, Phys. Rev. Lett. **81** (1998) 3591 [[hep-ph/9806530](#)].
- [90] G. Oderda, *Dijet rapidity gaps in photoproduction from perturbative QCD*, Phys. Rev. D **61** (2000) 014004 [[hep-ph/9903240](#)].
- [91] J. R. Forshaw, A. Kyrieleis and M. H. Seymour, *Super-leading logarithms in non-global observables in QCD*, JHEP **0608** (2006) 059 [[hep-ph/0604094](#)].
- [92] J. R. Forshaw, A. Kyrieleis and M. H. Seymour, *Super-leading logarithms in non-global observables in QCD: Colour basis independent calculation*, JHEP **0809** (2008) 128 [[hep-ph/0808.1269](#)].
- [93] M. Dasgupta and G. P. Salam, *Resummation of non-global QCD observables*, Phys. Lett. B **512** (2001) 323 [[hep-ph/0104277](#)].

- [94] M. Dasgupta, G. P. Salam, *Accounting for coherence in interjet $E(t)$ flow: A Case study*, JHEP **0203** (2002) 017. [[hep-ph/203009](#)].
- [95] A. Banfi, G. Marchesini and G. Smye, *Away from jet energy flow*, JHEP **0208** (2002) 006 [[hep-ph/0206076](#)].
- [96] A. Banfi, M. Dasgupta, *Problems in resumming interjet energy flows with k_t clustering*, Phys. Lett. **B628** (2005) 49-56. [[hep-ph/508159](#)].
- [97] Y. Delenda, R. Appleby, M. Dasgupta and A. Banfi, *On QCD resummation with $k(t)$ clustering*, JHEP **0612** (2006) 044 [[hep-ph/0610242](#)].
- [98] A. Kyrieleis and M. H. Seymour, *The colour evolution of the process $q q \rightarrow q q g$* , JHEP **0601** (2006) 085 [[hep-ph/0510089](#)].
- [99] M. Sjödal, *Color evolution of $2 \rightarrow 3$ processes*, JHEP **0812** (2008) 083 [[hep-ph/0807.0555](#)].
- [100] P. Nason, *A New method for combining NLO QCD with shower Monte Carlo algorithms*, JHEP **0411** (2004) 040 [[hep-ph/0409146](#)].
- [101] S. Frixione, P. Nason and C. Oleari, *Matching NLO QCD computations with Parton Shower simulations: the POWHEG method*, JHEP **0711** (2007) 070 [[hep-ph/0709.2092](#)].
- [102] S. Alioli, P. Nason, C. Oleari and E. Re, *A general framework for implementing NLO calculations in shower Monte Carlo programs: the POWHEG BOX*, JHEP **1006** (2010) 043 [[hep-ph/1002.2581](#)].
- [103] T. Sjöstrand, S. Mrenna and P. Z. Skands, *PYTHIA 6.4 Physics and Manual*, JHEP **0605** (2006) 026 [[hep-ph/0603175](#)].
- [104] J. R. Andersen, L. Lönnblad and J. M. Smillie, *A Parton Shower for High Energy Jets*, [hep-ph/1104.1316](#).